Extraocular Muscles in Amyotrophic Lateral Sclerosis

Anton Tjust

Department of Integrative Medical Biology
Department of Clinical Sciences, Ophthalmology
Umeå 2017

Cover illustration: Cross-section of the medial rectus muscle from an ALS donor. The basement membranes of myofibers, nerves and blood vessels are labeled with an antibody against laminin and appear grey. Myofibers containing myosin heavy chain slow appear green and myofibers containing both myosin heavy chain slow and slow tonic appear yellow.

Dedicated to Greta Sonnsjö – my great grandmother and first scientific mentor

Table of Contents

Abstract

Amyotrophic lateral sclerosis (ALS) is an incurable neurodegenerative disease of motor neurons characterized by muscle paralysis and death within 3-5 years of onset. However, due to unknown mechanisms, the extraocular muscles (EOMs) remain remarkably unaffected. The EOMs are highly specialized muscles that differ from other muscles in many respects, including innervation and satellite cells (SCs). Understanding whether these factors play a role in the relative sparing of EOMs in ALS could provide useful clues on how to slow down the progression of ALS in other muscles.

The EOMs and limb muscles from terminal ALS patients and age-matched controls as well as the commonly used SOD1^{G93A} ALS mouse model were studied with immunofluorescence. Antibodies against neurofilament and synaptophysin were used to identify nerves and neuromuscular junctions (NMJs); against Pax7, NCAM, MyoD, myogenin, Ki-67, dystrophin and laminin, to identify SCs and their progeny in EOMs and limb muscles. The proportion and fiber size of myofibers containing myosin heavy chain (MyHC) slow tonic and MyHC slow twitch were also determined in human EOMs.

The abundance of SCs differed extensively along the length of control human EOMs, being twice as abundant in the anterior portion. Pax7-positive cells were also detected in non-traditional SC positions. EOMs from terminal ALS patients showed similar numbers of resting and activated SCs as the controls. In limb muscles of ALS patients, the number of resting and activated SCs ranged from low (similar to normal aged, sedentary individuals) to high numbers, especially in muscles with long duration of disease and varied between the upper and lower limbs. The EOMs maintained a high degree of innervation compared to hindlimb muscles of symptomatic SOD1^{G93A} mice. MyHC slow tonic fibers were less abundant in ALS patients than in controls. The change seemed more pronounced in bulbar onset patients, and in this group of subjects only, there was a strong association between decline in MyHC slow tonic fibers and age of death. Notably, the decline in MyHC slow tonic fibers was unrelated to disease duration.

Our data suggested that SCs play a minor role in the progression of ALS in general and in the sparing of the EOMs in particular. The generally preserved innervation in the EOMs of G93A mice may reflect distinct intrinsic properties relevant for sparing of the oculomotor system. Even though the EOMs are relatively spared in ALS, MyHC slow tonic myofibers were selectively affected and this may reflect differences in innervation, as these fibers are multiply innervated.

Abbreviations

ALS	Amyotrophic lateral sclerosis
CNS	Central nervous system
CSA	Cross-sectional area
C9orf72	Chromosome 9 open reading frame 72
DAPI	4',6-diamidino-2-phenylindole
EOM	Extraocular muscle
MIFs	Multiply innervated fibers
MyHC	Myosin heavy chain
MyHCI	Slow twitch myosin heavy chain
MyHCsto	Slow tonic myosin heavy chain
NCAM	Neuronal cell adhesion molecule
NMJ	Neuromuscular junction
Pax7	Paired box protein 7
PBS	Phosphate buffered saline
PBST	Phosphate buffered saline + 0.05% Tween 20
RRX	Rhodamine Red X
SCs	Satellite cells
SIFs	Singly innervated fibers
SOD1	Superoxide dismutase 1
Wt	Wild-type

Svensk sammanfattning

Amyotrofisk lateralskleros (ALS) är en obotlig neurodegenerativ sjukdom som främst påverkar kroppens viljestyrda motoriska nervceller. ALS leder till förlamning, muskelförtvining och slutligen döden genom andningssvikt, vanligen inom tre till fem år efter sjukdomsdebuten. Av okända anledningar så bibehålls ögonmusklernas funktion mycket bättre vid ALS i jämförelse med andra muskler och är hos merparten av patienter i stort sett opåverkade. Ögonmusklerna är mycket specialiserade muskler som skiljer sig från andra muskler i kroppen på flera sätt, bland annat genom deras unika nervförsörjning och genom de satellitceller – muskelspecifika stamceller, som finns i dem. En ökad förståelse för hur dessa faktorer inverkar på ögonmusklernas motståndskraft vid ALS skulle kunna ge värdefulla ledtrådar till hur man skulle kunna sakta ned sjukdomens fortskridande i andra muskler vid ALS.

Ögonmuskler och extremitetsmuskler från avlidna ALS-patienter och åldersmatchade friska kontroller, tillsammans med transgena möss med den sjukdomsalstrande mutationen $SOD1^{G93A}$, studerades genom immunfluorescens och efterföljande mikroskopering. Antikroppar mot molekylerna Pax7, NCAM, MyoD, myogenin, Ki-67, laminin och dystrofin användes för att identifiera satellitceller och deras dotterceller i ögonmuskler och extremitetsmuskler. Antikroppar mot neurofilament och synaptofysin användes för att identifiera nerver och neuromuskulära synapser hos transgena SOD1-möss. Antikroppar mot toniska (tonic) och ryckande (twitch) muskelmyosinkedjor användes för att bestämma proportionen av och storleken på dessa typer av muskelfibrer i ögonmuskler från avlidna ALS-patienter och friska kontroller.

Mängden satellitceller varierade mellan de främre och de mer bakre delarna i friska, humana ögonmuskler och var dubbelt så många i den främre delen av muskeln jämfört med den mellersta och bakre delen av muskeln. Celler som uttryckte satellitcellsmarkören Pax7 hittades även i icke-traditionella satellitcellspositioner i ögonmusklerna. Mängden satellitceller i ögonmusklerna från ALS-patienter var samma som hos friska kontroller. I extremitetsmusklerna hos ALS-patienter varierade mängden satellitceller mellan låga nivåer (liknande de hos friska åldrade, inaktiva individer) till höga nivåer, särskilt i muskler där sjukdomen fortskridit under lång tid. Dessutom varierade mängden satellitceller mellan övre och nedre extremiteter.

Hos symptomatiska SOD1^{G93A}-möss hade ögonmusklerna en mycket välbevarad innervation jämfört med bakbensmusklerna, där många neuromuskulära synapser saknade kontakt mellan nerven och motorändplattan.

Proportionen muskelfibrer med toniska muskelmyosinkedjor var lägre hos ALS-patienter jämfört med friska kontroller. Denna minskning var tydligare hos patienter där sjukdomssymtomen hade debuterat i tugg- och ansiktsmuskulaturen – så kallad bulbär ALS. Dessutom fanns det i den här gruppen, men ingen annan studerad grupp, en stark korrelation mellan nedgången i toniska fibrer och patientens ålder. Värt att notera är att minskningen av toniska muskelfibrer saknade korrelation med hur länge patienten hade varit sjuk i ALS.

Den generellt välbevarade innervationen i ögonmusklerna hos SOD1^{G93A}-möss kan spegla distinkta inneboende egenskaper hos ögonmusklerna som är av vikt för bevarandet av ögonrörligheten vid ALS.

Gällande satellitceller så antyder våra data att satellitceller och deras regenerativa kapacitet spelar en försumbar roll vid ALS i allmänhet och vid ögonmusklernas bevarande i synnerhet.

Slutligen, även om ögonmuskler generellt är välbevarade vid ALS så är toniska muskelfibrer märkbart påverkade och detta kan spegla skillnader mellan olika nervcellsgruppers känslighet vid ALS.

List of original papers

1: Lindström M*, Tjust AE*, Pedrosa Domellöf F
Pax7-positive Cells/Satellite Cells in Human Extraocular Muscles
Invest Ophthalmol Vis Sci 2015;56;6132-43

2: Tjust AE, Lindström M, Sjöström J, Andersen, PM, Brännström T,
Pedrosa Domellöf F
Satellite cells and other muscle progenitor cells in extraocular muscles
and limb muscles of ALS donors
[Manuscript]

3: Tjust AE, Brännström T, Pedrosa Domellöf F
Unaffected motor endplate occupancy in eye muscles of ALS G93A mouse
model
Front Biosci (Schol Ed) 2012;4:1547-55

4: Tjust AE, Danielsson A, Andersen PM, Brännström T, Pedrosa
Domellöf F
Impact of ALS on slow tonic myofiber composition in human extraocular
muscle
[Manuscript]

*= Lindström M and Tjust AE were joint first authors on this paper

All published papers were reproduced with the kind permission of the
copyright holders.

Introduction

Amyotrophic lateral sclerosis

Amyotrophic lateral sclerosis (ALS) is a neurodegenerative disease first described neuropathologically by Jean-Martin Charcot in 1869 [1]. The disease is characterized by a progressive loss of upper and lower motor neurons in the central nervous system (CNS). The loss of upper motor neurons in the cerebral cortex, especially pyramidal neurons in the precentral gyri [2], leads to a degeneration of the lateral corticospinal tracts of the spinal cord, hence the term "lateral sclerosis". The loss of upper motor neurons leads to a pathological increase in muscle tone (spasticity) and upon patient examination, exaggerated tendon reflexes. Concomitant to this, there is a loss of lower motor neurons in the anterior horns of the spinal cord. This leads to muscle wasting; hence the term "amyotrophic", fasciculations and inability to recruit muscle fibers, resulting in paresis and eventually, complete paralysis and loss of tendon reflex responses. [3].

Eventually, the loss of muscle function starts to impede the respiratory muscles, leading to respiratory failure. The vast majority of patients die as a consequence of this, usually from CO_2 retention or aspiration pneumonia. The median survival time of an ALS patient is approximately 2,5 years, but exceptions are common, with 5% of patients living for at least 10 years with the disease [3]. As of today, there is only one internationally recognized drug that is prescribed to prolong the survival of ALS patients – Riluzole. This drug prolongs the median survival by only 2 to 3 months [4].

The first symptoms of ALS and the subsequent progression usually follow a recognizable pattern. That is, the disease usually starts unilaterally in a hand or a foot, with the patient experiencing an unprecedented fumbliness and difficulties in fine motor skills. Or, in the case of the foot, it may be experienced as a foot drop, stumbling, or an unexplainable change in gait pattern. This initial disturbance then starts to progress in an anatomically predictable pattern, involving more and more adjacent myotomes. Initially, the disease usually progresses in a unilateral fashion, sparing the opposite side of the body. Eventually, however, the presenting symptoms that the patient experienced in one hand or foot start to appear on the contralateral side. At this stage, the patient exhibit signs of both upper motor neuron and lower motor neuron dysfunction, but as the disease wears on, the upper motor neuron symptoms usually become less and less noticeable in the affected regions; masked by the severe lower motor neuron dysfunction. This clinical picture is usually termed "Classical ALS" or "spinal onset ALS" [3].

In approximately 25% of cases, the disease initially manifests in the brainstem, in motor neurons responsible for the function of facial, masticatory and articulatory muscles [3]. These patients first experience problems with articulating words and difficulties with chewing and swallowing, termed "bulbar dysfunction". Later, these patients usually start exhibiting signs of upper motor neuron and lower motor neuron degeneration at the spinal level as well and hence this is referred to as "bulbar onset ALS" [3].

Most patients (90-95% of cases) have no known family history of ALS and are designated sporadic cases of ALS. In the remaining 5-10% of patients, there is a family history of ALS and these cases are referred to as familial ALS [3]. Mutations in several genes have been linked to familial ALS (and are occasionally found in sporadic cases) and most often the disease is inherited in an autosomal dominant pattern with a high penetration rate [5].

The most well-known gene associated with ALS is the superoxide dismutase 1 gene (SOD1) – the first gene linked to ALS [5,6]. SOD1 is a homodimeric enzymatic protein that catalyses the conversion of superoxide into hydrogen peroxide [7]. Disease inheritance mostly occurs in an autosomal dominant and rarely, autosomal recessive pattern. More than 160 mutations throughout the gene have been linked to familial and sporadic ALS and account for 10-20% of familial ALS cases and 1-2% of sporadic cases [5]. Another well-known gene associated with ALS is the "Chromosome 9 open reading frame 72" (C9orf72) gene [8]. ALS patients with mutations in C9orf72 exhibit a hexanucleotide (GGGGCC) repeat sequence that is expanded from the normally occurring 2-23 repeats to 700-1600 repeats [5]. One notable feature of C9orf72 expansions is that they can also lead to fronto-temporal dementia, an unusual type of dementia that mainly affects the executive and inhibitory cognitive functions of the brain [8].

Being the first gene associated with ALS, SOD1 mutations have been used to generate a number of transgenic animals. The most widely used and best characterized is the SOD1^{G93A} C57BL/6 mouse model [9]. This mouse strain carries multiple copies of a human SOD1 gene with the G93A missense mutation in its genome. The disease manifests in a number of ways in this model. First, the weight gain of transgenic animals, especially males, is slower than wild-type (Wt) littermates from an early age and they never catch up with non-transgenic mice [10]. Rotarod and hanging wire test, classic motor performance tests, show that motor performance starts to decline around 80 to 90 days of age [10]. However, other more sensitive tests such as high-speed forced treadmill tests reveal that impaired motor function can be seen at 45 days of age. Around 90 days of age, weight curves start to level out

and turn downwards. Coinciding with decreased rotarod and hanging wire performance, this is considered as "disease onset". Eventually, mice reach the terminal stage of the disease, characterized by hind limb paralysis, kyphosis, and difficulties with cleaning and feeding themselves. This stage usually occurs around 135 days of age and prompts the sacrifice of the animal [9,10]. Upon histological examination, these terminal animals show the same loss of upper and lower motor neurons, coupled with typical changes in the skeletal muscles, that is normally present in samples from human ALS patients [9,11].

One remarkable hallmark of ALS is that some motor neurons seem to partially or completely escape the degeneration that occurs in the rest of the CNS. Such notable examples are the motor neurons of the oculomotor nuclei supplying the extraocular muscles (EOMs) [12] and the motor neurons of Onuf's nucleus that supply the striated external anal sphincter muscle [13]. Also, while not spared, the disease seems to progress at a slower pace in the preganglionic sympathetic motor neurons of the thoracic spinal cord [14,15]. These exceptions provide an opportunity to explore the mechanisms of sparing in these parts of the motor system and could hopefully guide future strategies in the search of drug targets that could slow down the progression of ALS. In this thesis, the main focus will be on the sparing of the EOMs, a group of muscles with numerous distinguishing qualities that set them apart from other types of muscles, qualities that might play a role in their relative sparing in ALS.

Extraocular muscles

The EOMs of vertebrates are ancient muscles, even phylogenetically older than terrestrial life on earth, pre-dating it by millions of years given that EOMs were present already at the divergence between lampreys and jawed fish 462 to 535 million years ago [16]. In humans and other tetrapods, each eye is supplied by six EOMs, consisting of four recti muscles (the medial, lateral, superior and inferior recti) and two oblique muscles (superior and inferior obliques). Together, they control the position of the globe within the orbita so that objects of interest can be imaged on the retinal fovea. The innervation of the EOMs of each eye is divided between motor branches of three cranial nerves: the oculomotor nerve, which is the third cranial nerve supplying rectus medialis, rectus superior, rectus inferior and obliquus inferior; the trochlear nerve, which is the fourth cranial nerve, supplying the superior oblique and the abducens nerve, which is the sixth cranial nerve supplying the lateral rectus. The EOMs are organized into antagonistic pairs that direct the globe in opposite orientations. The medial and lateral recti confer horizontal movements, so that the medial rectus adducts the globe

and the lateral rectus abducts the globe. The orbital cavities have an outward angle in relation to the midline of the skull. Therefore, the remaining EOMs, the superior and inferior recti and the oblique muscles, have diagonal force angles and convey depressing or elevating movements as well as torsional movements upon contraction [17].

The movements of the globe are further complicated by not only being the summation of aforementioned movements (adduction/abduction, elevation/depression, intorsion/extorsion) but also by being generated on the basis of different neurological motor patterns. One of the most fundamental functions of the EOMs is to stabilize the image falling on the retina, which is supported by reflexes such as the vestibulo-ocular reflex. Beside these non-voluntary movements, the gaze can be willingly oriented towards a new target (saccades) or locked on a slowly moving target, following it in an uninterrupted arc (smooth pursuit movements). Another movement of distinct importance for humans and other primates is vergence, which realigns the two foveae of the eyes so that the two images are as identical as possible [17].

These motions are executed by the myofibers of the EOMs, and with the constant activity of the EOMs, even during sleep, EOM myofibers have evolved specifically to cope with this extreme degree of activity. Most EOM myofibers display a very high oxidative and glycolytic capacity [18], coupled with the most extensive vascularization and highest blood flow of all voluntary muscles even during the simple task of looking straight ahead [19,20]. Rather than alternating between complete relaxation and contraction state in response to visual activity, the EOMs are constantly active, with motor neurons in the oculomotor nuclei sending trains of action potentials at rates that can be tenfold higher than those in limb muscles. Also, these motor neurons innervate very small motor units, in the range of 7 to 25 myofibers per motor neuron [21,22], compared to the 300 to 2000 myofibers normally innervated by individual lower motor neurons in the spinal cord [23].

The terminals of oculomotor neurons mainly take the form of the common "en-plaque" endings of the motor axon, forming a single neuromuscular junction (NMJ). However, a subset of myofibers in the EOMs are innervated at regular intervals along the length of the myofiber by small NMJs of simpler structure referred to as "en-grappe" endings [24]. Based on the electrophysiological properties and innervation of myofibers in the EOMs, they have been characterized as singly, en-plaque innervated fibers (SIFs) and multiply, en-grappe innervated fibers (MIFs) [25]. However, MIFs in the orbital layer generally have, in addition to the en-grappe endings along the myofiber, an NMJ near the middle portion of the muscle that is

more similar to ordinary en-plaque NMJs [26]. Myofibers can be further divided according to their relative position within the EOM. On cross-section of recti muscles, a layer of very small, densely packed myofibers is present as a crescent towards the orbital wall. This is referred to as the orbital layer. The remaining part of the muscle is occupied by larger myofibers, forming the global layer. Both layers harbor SIFs and MIFs, but these fibers differ between the layers both in terms of electrophysiological and histochemical properties.

Beyond the categorization based on innervation and layer localization, myofibers are further classified according to their myosin heavy chain (MyHC) composition [27]. MyHCs are the main contractile proteins present in the myofibrils. The MyHC isoform(s) present in a myofiber has a large influence on its tensile strength, contractile velocity, relaxation time and metabolic preference [27]. In human limb muscles, myofibers typically contain MyHCI – a slow twitch -type myosin, or alternatively, MyHCIIA or MyHCIIX – two fast twitch-type myosins [27]. Before and shortly after birth, other so-called developmental MyHC isoforms are normally expressed in developing myofibers. These are referred to as MyHC embryonic and MyHC neonatal [28]. These MyHC isoforms are eventually replaced by the mature MyHC isoforms, but when myofibers are damaged and undergo repair, they transiently re-express the developmental isoforms [28]. The myosin composition of myofibers is partially influenced by the embryonic lineage of the myoblasts that originally formed them, and also by the neuronal input they receive from the motor neuron that innervates them[29]. In the EOMs, the repertoire of MyHC isoforms present in mature myofibers is wider than all other muscles and includes all muscle-related MyHCs present in the body [30]. This includes, besides the most common MyHC isoforms in skeletal muscles (MyHCI, MyHCIIA and MyHCIIX) more unusual MyHC isoforms, such as MyHC extraocular (an EOM-specific myosin in most mammals), MyHC slow tonic (MyHCsto), MyHC α-cardiac, MyHC Slow B as well as the aforementioned developmental MyHC isoforms (MyHC embryonic and MyHC neontatal) [30-33]. Limb myofibers typically contain one or two MyHC isoforms [27]. In contrast, human EOM myofibers typically contains several MyHC isoforms [33] and in rabbit EOMs, up to six different MyHC isoforms in one myofiber have been demonstrated [34], making a clear-cut categorization of EOM myofibers difficult. In addition, the MyHC content of individual myofibers varies along their length [33]. The MIFs present in the orbital and global layer that contain MyHCsto and/or MyHCI do seem to form a group of their own, though there are some differences even within that group regarding co-expression of MyHC α–cardiac and the developmental MyHC isoforms [33,34]. The remaining myofibers, the SIFs, typically contain MyHCIIA, MyHC extraocular or a mixture of those MyHC isoforms, forming

a continuum, often together with one of the less common MyHC isoforms [33]. Even though the MyHC composition of the human EOM fibers is very complex and varies along the length of the myofibers, three major fiber groups can be separated: SIFs mainly containing the fast-twitch MyHCIIA isoform, MIFs containing MyHCsto and/or MyHCI and SIFs lacking both MyHCIIA and MyHCsto/MyHCI and containing predominantly MyHC extraocular [33].

The EOMs differ fundamentally from other muscles in the body and constitute a separate allotype. The most intriguing property of the EOMs is that they are differentially affected in a number of neuromuscular diseases [35]. They are selectively spared in Duchenne's muscle dystrophy [36], merosin-deficient muscular dystrophy [37,38] and ALS [39,40]. Furthermore, they are preferentially vulnerable in myasthenia gravis and Miller-Fischer syndrome [35], the later being a possible consequence of the abundance of specific ganglioside epitopes at the NMJ of the EOMs, but not at the NMJs of limb muscles [41]. The EOMs separate lineage and unique characteristics are reflected in their transcriptome, which deviates considerably from limb muscles [42,43]. In humans, a two-fold differential expression between EOMs and limb muscles has been noted for approximately 340 genes and encompasses differences in intracellular cell signaling, ionic homeostasis and numerous constituents of the basement membrane [42].

Extraocular muscles and ALS

Despite the involvement of virtually all voluntary muscles in ALS, it has long been noted that eye motility usually remains preserved throughout the course of the disease [44]. Exceptions to this have been reported, mostly in the form of sporadical case reports [39,45,46], but also in a case series after the introduction of permanent respirator treatment for ALS patients in Japan [47,48].

Post-mortem examination of one case with complete external ophthalmoplegia revealed a profound loss of motor neurons and gliosis in the oculomotor nuclei [45]. In referring to this case in 1983 and adding another patient, Cohen et Caroscio [39] pointed out the importance of separating those ALS patients that exhibit lesions in the brainstem, limiting the actual recruitment of myofibers, from those patients demonstrating supranuclear lesions of the cortico-oculomotor pathway. Reviewing the available case reports, the patients with eye motility disturbances seem to fall into the later category, with difficulties/inability to generate voluntary eye movements, but with a preserved ability to move the eye upon corneal stimulation [47]. This suggests that the oculomotor system of the brainstem in most patients, even

those with ophthalmoplegia, is relatively well preserved and due to a loss of upper motor neurons. Indeed, an early neuropathological survey of 53 ALS cases [2] reports that cellular changes of the oculomotor nucleus were present on post-mortem examination only in four cases, but no clinical disturbance of eye motility was noted for these patients in that report. A later study [12] looked specifically at the oculomotor, trochlear and the abducens nuclei of 27 ALS patients and reported that only two patients displayed any motor neuron loss and out of these, only one, a patient with overt ophthalmoplegia after two years of respirator use, showed definite signs of motor neuron loss. In contrast to neuropathological findings, functional investigations of eye motility of ALS patients show that most patients display a slight, but still measurable degree of eye motility impairment [49,50].

Consistent with the findings in the CNS that lower motor neuron loss is very rare in the oculomotor nuclei of ALS patients, the first thorough analysis of EOMs from a cohort of deceased ALS patients revealed that the EOMs of these patients were very well preserved in comparison to the pathological changes present in their limb muscles [40]. This study revealed that the relative sparing of eye motility is also present at the muscle-level of ALS patients but also that the EOMs display a heterogeneous involvement in most patients. Typically, EOMs of ALS patients display little changes in myofiber size, proportion of connective tissue and little to no myofiber grouping. However, individual EOMs occasionally exhibit more dramatic changes such as changes in MyHC isoform content, fiber grouping, hypertrophic changes and an increased presence of nerve fascicles or connective tissues [40]. Remarkably, these changes appear to be localized, as other EOMs on the ipsi- or contralateral side can be just as well preserved as is normally the case in ALS [40]. These findings points out that the sparing of the EOMs is relative and far from fully understood. However, understanding the basis for the relative sparing of the EOMs could provide clues to processes that could be of importance when devising strategies for slowing down the progression of ALS in other parts of the motor system.

Satellite cells

The relative sparing of the EOMs that has been demonstrated in relation to ALS has also been demonstrated in other neuromuscular diseases [35]. In Duchenne and Becker muscle dystrophy, the sparing of the EOMs has been suggested to stem from an enhanced regenerative capacity of their satellite cells (SCs) [51,52]. SCs are muscle progenitor cells, found between the sarcolemma and basement membrane of a myofiber [53]. In adults, SCs are normally in a quiescent state. However, in response to different stimuli, SCs

become activated and enter the cell cycle and proliferate to produce new myoblast [54]. These are able to either re-enter a quiescent state to maintain or increase the pool of SCs or differentiate to post-mitotic myocytes capable of fusing and contributing to myofiber repair, new myofiber formation or the addition of a new myonucleus to a growing myofiber [55-57]. SC behavior is at least partly regulated by factors that are also expressed during embryonic muscle formation and several steps in SC activation bear resemblance to primary and secondary myogenesis [58,59]. Activated and differentiating SC progeny are distinguishable from quiescent SCs by the expression of myogenic regulatory factors, such as MyoD and myogenin (Figure 1).

SCs increase in number throughout childhood and adolescence, contributing new myonuclei to growing myofibers [60]. The quantity of SCs decreases with aging [60,61], but this decrease seems to be, at least partially, reversible with exercise [62]. There is also a difference in SC quantity between different muscles and fiber types [63,64], possibly related to differences in the duration and intensity of loading put on that muscle, as increase of SC content in response to exercise is preferentially located to the most utilized fiber type [65,66]. SCs in the EOMs have been reported to be more numerous than in other muscles and suggested to be highly mitotically active compared to limb muscles [67,68]. This has been suggested to result in constant myofiber remodeling, and this remodeling is thought to confer the resistant traits of EOMs [52] to neuromuscular diseases. In addition, SCs from EOMs have been shown to have a superior proliferative capacity in vitro and can expand considerably when injected into limb muscles [69].

Several recent studies have implicated that SCs from limb muscles in ALS animal models [70-72] and patients [73,74] are highly activated, express markers of differentiation, and are speculated to possibly become exhausted in advanced ALS due to an excessive number of replicative cycles [71,74], together with a proposed cell-autonomous effect of ALS on SCs that is independent from the denervation that follows with the disease [70,71,73]. This suggestion derives from the observation that some effects of ALS are muscle-specific rather than neuron-specific and that muscle-restricted expression of the G93A SOD1-mutation leads to a motor dysfunction phenotype [75,76]. Furthermore, SCs appears to serve an important role in the reestablishment of denervated NMJs, as depletion of Pax7-positive cells leads to less successful reinervation after nerve lesions [77]. The only previous study that investigated SCs of human ALS patients in their natural environment was conducted on patients with one year of disease duration, which might be too early to detect the long-term effects of ALS on the SC pool [78].
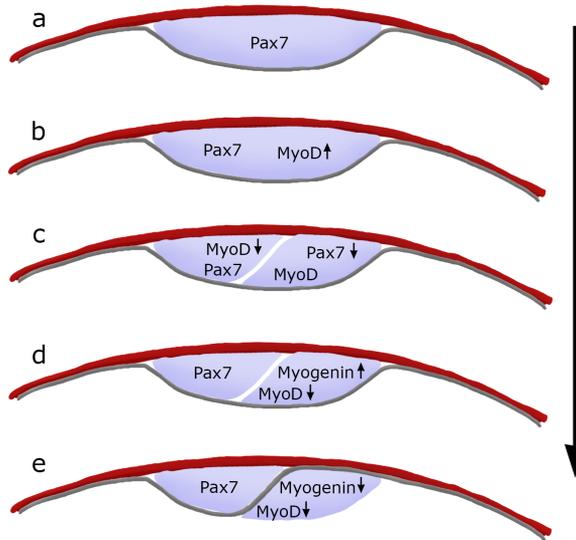
Figure 1.

   Schematic illustration of Pax7, MyoD and myogenin expression patterns during SC activation and differentiation. Quiescent SCs (a) express Pax7. Upon stimuli (b), the cell is activated to proliferate, MyoD is up-regulated. After mitosis (c), non-differentiating cells will down-regulate MyoD and retain Pax7. Continued expression of MyoD and down-regulation of Pax7 will lead to differentiation (d) and up-regulation of myogenin. Next, the cell will fuse with the sarcolemma (e) and become a myonucleus. Afterwards, myogenin and MyoD will become down-regulated.

   The early studies on SCs were originally based on electron microscopy techniques, where SCs were identified on the basis of their localization inside the basement membrane but outside of the sarcolemma (plasma membrane) of the myofiber [53]. With the advent of antibody labeling it became possible to characterize SCs based on their molecular properties [79,80]. Quiescent and activated SCs were found to express the transcription factor paired box gene 7 (Pax7), which is important for the basic function of SCs, as well as a specific marker for SCs in muscles of different species [80-82]. Subsequent work by our group has resulted in a refined multiple marker method that enables a reliable identification and characterization of SCs and other muscle progenitor cells in human muscles, as well as the markers they express during activation and differentiation [82,83].

In light of the proposed role of SCs in the unique disease resistance of EOMs and their suggested impairment in ALS, one goal of the current thesis was to use the aforementioned methods to investigate the abundance of resting and activated SCs in EOMs and limb muscles. The investigation involved the SCs of EOMs to elucidate their possible role in EOM sparing in ALS as well as the SCs of skeletal muscles, in order to investigate whether signs of disturbed SC function, as previously reported in cell cultures and animal models, was observable in situ.

While patient material provides valuable information about ALS as it manifests in humans, the heterogeneity of patients with regard to site and age of onset, underlying genetic causes and survival length means that it can be difficult to draw conclusions regarding step-wise processes. The G93A mouse model, while only being a model of the disease and not necessarily reflecting the whole breadth of ALS as it manifests in humans, overcomes some of the problems of patient-based studies and allows for investigations that otherwise would not be possible. Using the G93A mouse, it has been shown that there is a striking discrepancy between observable loss of motor neurons and manifestations of denervation at the muscle level [84]. A previous study analyzing the NMJ, axons and neuronal soma of G93A mice at different time points shows that denervation, loss of motor axons and loss of motor neurons, appear through a distal-proximal progression sequence so that signs of denervation on the NMJ-level become detectable around 47 days of age, major loss of axonal fibers is seen in the ventral root level around 80 days of age and motor neuron loss in the spinal cord is noticeable at 100 days of age [84]. Furthermore, in the late-stage, but not yet terminal animals, there is a small increase of small-caliber axons in the ventral root and a slight improvement of the innervation ratio, suggesting that some of the remaining motor neurons are attempting to re-innervate myofibers of more sensitive motor units [84]. Based on this, it was suggested that ALS is a neurodegenerative disease characterized by a "dying-back" phenomenon [84,85], and that ALS and other motor neuron diseases should be regarded as axonopathies where the first signs of disease manifest at the NMJ level [85]. Furthermore, vacuolization of mitochondria, a recurrent finding in afflicted cells in ALS, can be detected as early as 25 days of age in the presynaptic NMJ of SOD1G93A mice [86,87]. Also, muscle mitochondrial defects can be seen in symptomatic ALS patients [88] and weight loss, denervation and motor neuron death have been shown to be inducible in mice through a muscle-restricted impairment of mitochondrial efficiency by overexpressing mitochondrial uncoupling protein 1 [89].

The relative sparing of EOMs in ALS raises the question whether the "dying-back" phenomenon is absent, delayed or somehow overcome by a

highly successful re-innervation of NMJs in these muscles. As retraction of the terminal axon at the NMJ is an early manifestation of muscle-motor neuron disturbance, NMJ assessment is a good indicator of disturbances in the relationship between myofibers and their motor neurons. Therefore, one goal of the thesis was to investigate whether contacts between the terminal axon and motor endplates were preserved in the EOMs of the SOD1[G93A] mouse model, as a possible mechanism behind the sparing of the EOMs in ALS.

As mentioned earlier, the human EOMs are only mildly affected at the end-stage of ALS and important variation was seen between donors [40]. Furthermore, there were changes in the MyHC isoform composition in the EOMs of terminal ALS patients [40]. Previously, it has been recognized that different types of motor neurons in the spinal cord are affected in a predictable pattern during the progression of ALS in transgenic SOD1 mice[90,91]. The most sensitive motor neurons are the fast-fatigable motor neurons that innervate large motor units containing MyHCIIx myofibers. These are the first to lose contact with their respective muscle fibers, followed by motor neurons with intermediate characteristics called fast fatigue-resistant motor neurons that innervate somewhat smaller motor units made up of fast MyHCIIA myofibers. The most resistant motor neurons are those innervating slow (MyHCI) myofibers, those adapted to low, continuous activity. This is reflected in the structure of the NMJs of these myofibers, where fast spinal motor neurons form large NMJs that are rich in mitochondria on the pre- and postsynaptic side, have a high density of vesicles in the terminal axon and deep, elaborate folds. In contrast, slow spinal motor neurons form smaller, simpler NMJs with more moderate vesicle densities and fewer mitochondria [92]. This could indicate that fast motor neurons are more vulnerable because of a higher demand on the axonal transportation mechanisms responsible for maintaining such NMJs, and indeed disruption of axonal transport first becomes detectable in the axons of fast motor neurons in the SOD1[G93A] mouse model [93].

In the EOMs, slow MyHCI-containing fibers also co-express MyHCsto and are the multiply innervated fibers (MIFs) present in the orbital and global layer. With motor neurons innervating slow myofibers being notably resistant among spinal motor neurons, it would be of interest to study the involvement of slow myofibers in the EOMs in ALS patients. Previous investigation into MyHC composition of EOMs from ALS patients showed that myofibers with MyHCsto are decreased in the global layer, but that MyHCI expression is preserved. However, high variability between donors and limited material prevented any further quantification [40]. MIFs of the EOM and their motor neurons are also of interest since, whereas different

classes of spinal motor neurons are difficult to separate from one another without concurrent electrophysiological investigations, MIF-innervating motor neurons are located in an anatomically separated niche of their respective nucleus and express other surface markers than their SIF-innervating neighbors [94-96]. This means that any changes, adaptive or pathological, at the myofiber level can be correlated to changes at the motor neuron level.

With these factors in mind, one of the aims of the thesis was to explore the involvement of MIFs in ALS, using antibodies against MyHCI and MyHCsto as markers for these myofibers.

Aims of the thesis

To better understand the relative sparing of extraocular muscles in ALS, we investigated aspects of the EOMs that set them apart from limb muscles, with the aim of answering the following questions:

- What is the normal content of muscle progenitor cells in control human EOMs?

- Is the number of muscle progenitor cells evenly distributed along the length of the EOMs?

- Does the number of muscle progenitor cells in EOMs differ between ALS patients and controls?

- Does the number of SCs in limb muscles differ between ALS patients and controls?

- Are there differences between individual muscles and between healthy controls and afflicted donors in the abundance of differentiating muscle progenitor cells?

- Are there signs of depletion of SCs and other muscle progenitor cells in ALS patients with a protracted disease course?

- Is loss of innervation at the neuromuscular junction present in the EOMs of the SOD1^{G93A} mouse model?

- Is the proportion of MyHCsto myofibers affected in terminal ALS patients?

- Are changes in MyHCsto myofiber composition associated with the clinical characteristics of the patients?

Materials and methods

Animal models

Two lines of transgenic mice carrying mutated human SOD1 genes were used. The transgenic mice featured in paper 3 are heterozygous carriers of the G93A mutation [9], the most ubiquitous animal model used worldwide to study ALS. In the pilot study leading to paper 3, a small number of transgenic mice homozygous for SOD1 with the D90A translocation were analyzed together with the G93A mice. The animals were housed in cages at the animal house facilities at Umeå University and provided water and chow ad-libitum. The transgenic lines were bred with permission from the Swedish Board of Agriculture and the experiments were performed with approval from the Ethics committee on animal experiments in Umeå in accordance with the European Communities' Council Directive (86/609/EEC). Animals were inspected daily and when any of the terminal stage criteria were met, animals were sacrificed with a bolus dose of intraperitoneal barbiturate mixed with sodium chloride. Controls for either mouse line were littermates that did not carry the transgenic allele.

Human muscle samples

ALS patient donor material was collected at autopsy. Informed consent of participation was always retrieved from close relatives and from the patient prior to death whenever possible, in agreement with the Swedish Transplantation Law (SFS 1995:831), with permission from the Regional Ethical Review Board in Umeå and adhering to the tenets of the declaration of Helsinki. Patients were diagnosed according to the EFNS guidelines. Control samples were obtained post-mortem from age-matched donors without any known history of neurodegenerative disease to minimize confounding effects of general aging on interpretation of our findings, with ethical permission. A list of the patient and control donors is provided in Table 1. In addition, an aborted fetus (19th week of gestation), collected with ethical permission as above, was used as a positive control for some stainings in paper 2.

Muscle collection

EOMs and hind limb muscles (extensor digitorum longus, tibialis anterior, soleus and gastrocnemius) from mice were collected immediately post-mortem.

Table 1 – Clinical characteristics of ALS patients

Patient	Sex	Age at onset	Site of onset	Disease duration (months)	Age at death	Disease mutation(s)	In Paper
1	M	48	Leg	317	74	SOD1^{D90A} homozygous	II, IV
2	F	52	Leg	131	63	SOD1^{D90A} homozygous	II, IV
3	F	53	Hand	12	54	C9orf72	IV
4	M	58	Leg	9	59	C9orf72	IV
5	F	60	Hand	13	61	No known	IV
6	M	62	Hand	58	66	No known	IV
7	M	67	Leg	35	69	C9orf72	IV
8	M	69	Hand	16	70	No known	II, IV
9	F	72	Hand	10	73	SOD1^{A4V} heterozygous	IV
10	M	77	Hand	30	79	No known	II, IV
11	F	79	Bulbar	11	80	No known	II, IV
12	F	55	Bulbar	34	58	No known	II, IV
13	M	55	Bulbar	42	59	VAPB S160del	IV
14	M	60	Bulbar	64	65	No known	IV
15	F	63	Bulbar	13	64	No known	IV
16	M	64	Bulbar	13	65	No known	II
17	F	64	Bulbar	58	69	No known	IV
18	M	68	Bulbar	33	70	C9orf72	II
19	F	71	Bulbar	35	74	C9orf72	IV
20	M	75	Bulbar	17	77	No known	IV

Age of onset and age of death reported in full, lived years. Disease duration is calculated from reported onset of symptoms, rounded to full months.

EOMs from patient donors were collected by a supraorbital approach after removal of the brain. The roof of the orbita was excised and the accessible muscles (superior oblique, superior rectus, lateral rectus and medial rectus) were excised from the orbita on each side, cutting as close to proximal and distal insertions as possible. EOMs from control donors were taken through an anterior approach.

Limb muscle samples (biceps brachii, vastus lateralis and gastrocnemius muscles) from either group of donors were taken through skin incisions overlying the mid-belly portion of the muscle.

Each limb muscle sample was oriented, any fascia or fat removed, and the sample was cut into appropriately sized pieces and mounted for cross-section on cardboard with OCT cryomount (HistoLab Products AB, Gothenburg, Sweden). The EOM samples were carefully oriented longitudinally and mounted on cardboard wrapped in aluminum foil with OCT cryomount. Thereafter, samples were snap-frozen in propane chilled with liquid nitrogen and stored at -80°C before sectioning. Longitudinal EOM samples were later brought to -23°C, cut with chilled razor blades and remounted for cross sectioning of the anterior, middle and posterior portions. The samples were sectioned with a Leica CM3050 cryostat (Leica Biosystems, Nussloch, Germany). Section thickness varied between 5-7 μm, depending on the protocol and structures of interest. Muscle sections for confocal microscopy (Paper 1), were 30μm thick. Sections were either collected on gelatin-coated glass slides or, in the case of thick sections, on Superfrost plus adhesion slides (Gerhard Menzel GmbH, Braunschweig, Germany).

Immunofluorescence

To visualize proteins of interest, well-characterized primary antibodies, along with secondary antibodies conjugated with fluorescent proteins were used. Please see each paper for further details on the specific antibodies used. In general, the muscle sections were treated as follows: slides were brought to room temperature to air-dry for 15-20 minutes. Afterwards, slides were rehydrated in phosphate-buffered saline (PBS) for 3 times 5 minutes. For stainings where nuclei were visualized, this step was preceded by a post-fixation with 2% paraformaldehyde in PBS for 8 (thin sections) or 30 (thick sections) minutes. In sections treated with antibodies against nuclear antigens (Pax7, MyoD, myogenin and Ki-67), PBS washes were done with a 0,05 % admixture of Tween-20 (PBST) to enhance reagent penetration. In the case of thick sections, this was further amplified by a single 30 minute incubation with Triton X-100 after post-fixation but before the first PBST wash. After pre-treatments and washes, slides were incubated for 15 (thin sections) or 30 (thick sections) minutes with normal serum (either donkey normal serum or goat normal serum, depending on the subsequent secondary antibodies) to block non-specific binding. This was followed by incubation with the first primary antibody, usually overnight at +4°C. Next day, slides were brought to room temperature and washed in PBS (or PBST), followed by incubation with normal serum, as above. Then, secondary

antibodies with the same target species as the host species of the primary antibody were applied for 30 (thin sections) or 60 (thick sections) minutes at +37°C. Afterwards, slides were rinsed and incubated with normal serum again, followed by incubation with a new primary antibody for 60 (thin sections) or 120 (thick sections) minutes. Normally, two primary antibodies from different host species were mixed for this incubation. These primary antibodies usually had epitopes localized on different structures, or had been tested separately to exclude significant epitope competition. In the case of paper 3, we mixed primary antibodies against neurofilament and synaptophysin so that the whole terminal axon could be visualized. Otherwise, the two primary antibodies were one mouse monoclonal antibody mixed with a polyclonal antibody against a different protein. After incubation, slides were rinsed again and incubated with normal serum, followed by incubation with a second set of secondary antibodies for 30 or 60 minutes. Afterward, slides were rinsed a final time in PBS (all protocols), mounted with Vectashield or Prolong gold mounting medium, either with or without 4',6-diamidino-2-phenylindole (DAPI), depending on the protocol. For all studies, protocols were tested with the parallel stainings of secondary antibody control sections, i.e. omitting one or several of the primary antibodies to evaluate the background staining of individual secondary antibodies. When possible, protocols were tested with positive controls, constituted by samples with a known high prevalence of the target protein. For example, in the case of paper 2, the MyoD and myogenin labeling was verified with muscle sections from an aborted 19-week old fetus, known to contain numerous proliferating and differentiating muscle progenitor cells.

Microscope analysis

The first analysis of slides was done within a week of staining, usually on the day the staining was completed. Slides were analyzed with a Nikon E800 fluorescent microscope or a Leica DM 6000B with a motorized table. For paper 3, images all visible motor endplates in the section identified with α-bungarotoxin, whether innervated or not, were captured with a camera. For paper 1, 2 and 4, individual images were captured across the whole cross-section to generate a high-resolution montage of the whole section. For quantification of SCs and MyHC-labeled fibers, a number of images were randomly sampled from the montage. Where data was stratified according to layer (orbital or global), the boundary between the orbital and global layer of that particular section was drawn on a low-resolution image. Thereafter, images were randomly sampled within each layer. For quantification of MyoD, myogenin or Ki-67-labeled nuclei, we found that only a small fraction of the total nuclei were labeled for these markers on a given cross-section. Therefore, these nuclei were quantified through careful investigation of each

whole cross-section with an x40 objective. The search for labeled cells was carried out systematically, searching the cross-section in overlapping lines across the section, so that the whole area was searched twice. In some cases, two separate investigators quantified the same section to ensure that all labeled nuclei were detected. Labeled nuclei were captured at x40 magnification for later classification of localization in relation to the sarcolemma and basement membrane.

Discrete quantification

The majority of quantitative estimates in the papers were based on proportions derived from discrete quantification of cells and structures in the captured images. In paper 3, all NMJs on a given section were analyzed and classified as either innervated or denervated, based on the presence or absence of a labeled terminal axon at the alpha bungarotoxin-labeled motor endplate. Whenever quantifications were based on randomized images from the whole cross-section, a counting frame was used for unbiased quantification [97].

Estimation of cross-sectional area (CSA)

To put other estimates in relation to myofiber size, image files were imported into Leica Qwin Standard V.3.5.1 (Leica microsystems Ltd. Heerbrugg, Switzerland). On the imported images, myofiber contours, as defined by laminin labeling, were traced with a digital pen, omitting myofibers that were obliquely sectioned, frayed, broken or lacking an intact basement membrane. Care was taken to only trace the contours of myofibers and none of the small blood vessels and nerve fascicles that are present in muscle tissue. These were identified based on their thicker basement membrane and the difference in background staining present in them. As above, a counting frame was used for unbiased quantification [97]. After every myofiber contour on an image had been traced, the CSA was calculated and exported to the SPSS Statistics software environment (IBM, Armonk, NY, United States).

Pax7-positive cells in nontraditional positions (Paper 1 and 2)

In EOMs of controls, but also patients, Pax7-positive cells were also found in other localizations beside the traditional SC position. To better understand their possible roles in EOM biology, Pax7-positive cells were classified into seven categories and quantified in the anterior, middle and posterior portions of the control donors. For further details, please see figure 5, paper 1. During the work on paper 2, these categories were simplified into

myofiber-associated and interstitial Pax7-positive cells so that a more powerful comparison between control and ALS EOMs could be carried out.

Satellite cell quantification (Paper 1 and 2)

SCs in EOMs were labeled with a previously established protocol combining two SC markers: NCAM (also known as CD56 and Leu-19) and Pax7. Cells expressing these two markers were present not only in the traditional SC niche, sharing basement membrane with its parent fibers, but also as a separate cell, attached with its own basement membrane to a parent fiber. Furthermore, cells expressing NCAM and Pax7 were found completely detached from any myofiber, in the interstitium. Also, a large proportion of myofibers exhibited a weak NCAM labeling throughout the cytoplasm, making it hard to delineate the NCAM labeling of the myofiber from that of SCs in some cases. Due to these two factors, NCAM-positive cells lacking Pax7, which are known to make up a very minor proportion of SCs in limb muscles [82], had to be omitted from the quantitative estimates as NCAM-positive Pax7-negative cells in the interstitium of the EOMs could also represent other cell types, such as Schwann cells. SCs in the EOMs were quantified with Pax7 as the primary marker, by summing up all Pax7-positive cells in randomly selected images from the orbital and global layers and dividing by the number of myofibers in those images. This forms the proportion Pax7/F. Also, the number of myonuclei in myofibers was noted, giving us the proportion of myonuclei per fiber (N/F) and Pax7 cells per myonuclei (Pax7/N). Also, since the myofiber CSA of each image was quantified, we could calculate the two-dimensional myonuclear domain, expressed as μm² per myonucleus.

In limb muscles (Paper 2), SCs in limb muscles were identified and quantified based on their Pax7 and NCAM labeling, in combination with their SC position in relation to the myofiber basement membrane. Also, myofibers and myonuclei were quantified. Mean CSA and myonuclear domain were estimated as above. As interstitial Pax7-positive cells were present but relatively few in limb muscles of ALS donors and controls, SC/F and SC/N, rather than Pax7/F and Pax7/N, were used for limb muscle estimates.

Proliferating and differentiating muscle progenitor cells (Paper 2)

To further understand the activity of muscle progenitor cells in EOMs and limb muscles, 9 EOMs (5 from ALS cases, 2 from controls), 11 biceps brachii (7 from ALS cases, 4 from controls), 5 vastus lateralis (all ALS cases) and 5

gastrocnemius muscles (all ALS cases) were treated with antibodies against MyoD, myogenin and Ki-67 to identify activated and differentiating muscle progenitor cells. For each section, all nuclei labeled with the aforementioned antibodies were captured at x40 magnification and classified according to the relation with the sarcolemma (MyoD and myogenin), the basement membrane and co-labeling with Pax7 (Ki-67 only). The sarcolemma was identified with antibodies against dystrophin and the basement membrane was identified with antibodies against laminin. Since Ki-67 is ubiquitous in all cells during active cell cycle, Ki-67 labeled nuclei were categorized based on whether they were found inside of, or sharing basement membrane with a myofiber, as there was a high likelihood that other labeled nuclei could represent other, miscellaneous cells. Only the former category, Ki-67 labeled nuclei in association with a myofiber, were used in relation to the total myofiber area (see below).

Estimation of proportion of total myofiber area (Paper 2)

To facilitate comparison in the abundance of activated and differentiating muscle progenitor cells between sections of variable area and connective tissue content, the cross-sectional area of the whole muscle section was calculated for each muscle sample where MoyD, myogenin and Ki-67 labeled nuclei were quantified. This was done by tracing the contours of the whole section on a montage of the whole sample cross-section in Photoshop. Large rifts, folded pieces of the section and major nerves, arteries and veins were omitted and the number of pixels in the image was noted. Based on the known pixel resolution of the images used for the montage, the pixels marked were converted into section surface area, expressed in square millimeters (mm²). The cross-sectional area of samples varied extensively, from just below 15 mm² to 173 mm², but the majority were 30-40 mm². Also, there was a notable difference in the proportion of area covered with myofibers between the biceps of controls and ALS patients. The difference in fibrosis and other connective tissue, while being a known manifestation of neuromuscular disease presented a statistical problem as tissues with high degree of fibrosis could potentially have their numbers of activated SCs diluted by large areas of non-myofiber tissue, which was not expected to be myogenically active. Therefore, each sample was corrected for both the whole cross-sectional area as well as the proportional area of myofibers. To account for different degree of fibrosis, 7–10 images from each sample were analyzed with an overlaid grid. Each grid consisted of 391 equally spaced points and each point was noted as either overlying the interior of a myofiber or other, non-myofiber structures. The proportion of total myofiber area was estimated by dividing the total number of points overlying myofiber content

with the total number of points analyzed for that particular muscle, as described in [97]. This constant was then multiplied with the total section surface area, giving the total myofiber area in mm². This was then used as a denominator for the total number of MyoD, myogenin or myofiber-associated Ki-67 labeled nuclei found in that section and expressed as number of labeled nuclei per mm² of total myofiber area.

Motor endplate occupancy (Paper 3)

All NMJs were identified on EOM and hind limb muscle sections from 6 transgenic SOD1[G93A] mice and 6 control littermates. To evaluate muscle innervation, a method used previously [84] was utilized to label pre- and postsynaptic parts of the NMJ and evaluate the presence of the terminal axon from innervating motor neurons. In each NMJ, the presence of absence of a terminal axon, as labeled by the combined neurofilament + synaptophysin antibodies, was investigated at x20 and x40 magnification. Since the NMJs are primarily localized as a band in the muscle midbelly, it was sometimes difficult to find a large amount of NMJs in the limb muscle specimens. Therefore, serial sections investigated until at least 50 NMJs had been identified. In the pilot study leading up to paper 3, longitudinal and cross sections were compared in terms of NMJ yield and NMJ classification reliability.

In addition, the general morphology of EOMs and limb muscles was investigated on cross-sections stained with haematoxilin and eosin.

Analysis of MyHC content (Paper 4)

In the study of MyHCsto, a number of images were randomly selected from the orbital and global layer until the total number of myofibers in those images exceeded 1800 for the global layer and 1500 for the orbital layer. In each image, the myofibers were classified as either labeled for MyHC slow tonic (MyHCsto), MyHC slow twitch (MyHCI), both MyHC slow tonic and slow twitch (MyHCI+sto) or unlabeled by these antibodies. Based on these quantities, the proportion of MyHCsto, MyHCI and MyHCI+sto fibers to the total number of myofibers was calculated for each layer. Based on the images used for proportion estimates, images were randomly selected for CSA assessment until at least 180 myofibers in the global layer and 130 myofibers in the orbital layer labeled for either MyHC had been assessed.

Statistics

Statistical anal yses for paper I were carried out in StatView Software (SAS, Cary, NC, United States) but subsequently re-analyzed in SPSS (IBM, Armonk, NY, United States). SPSS was subsequently used for all data in the other papers included in the thesis. For statistical tests, differences between conditions, groups or within subjects were considered significant when $p<0.05$. All estimates were evaluated with regard to their distribution, both with statistical tests such as Shapiro-Wiks and visually with graphs, looking for excess skew, kurtosis or prominent outliers.

For independent group comparisons with normal distributions, student t-tests were used. In the case of non-normal distributions, Mann-Whitney U test was used. For comparisons with more than two independent groups, one-way ANOVA was used. In paper 3, there were no multiple comparisons, eschewing the need for correction of p-values. In paper 1, Sidak post-hoc correction was done to compensate for the increased family-wise error rate. As multiple parts of the EOM were tested, a Mauchly's test of sphericity was done, rendering an insignificant result. In paper 4, the study was conducted with a clear hypothesis in mind. Therefore, contrast tests were done for comparisons of proportion between groups of subjects, rather than pairwise comparisons with posthoc tests. Also, the distribution of MyHCI+sto proportion was not normal in the orbital layer. To overcome this, we ran the One-way ANOVA as a bootstrap with 8000 runs. In the study, comparisons between the CSA of different types of fibers and myofibers of different EOM layers were done with a Wilcoxon signed-rank test.

The regression analysis in paper 4 was done as a linear regression with age of death, age of onset and disease duration as dependent outcomes to the independent outcome "proportion of MyHCI+sto in the global layer". To ensure validity, the standardized residuals were tested for their distribution, and probed for outliers (standardized residuals exceeding 1,96). Also, Cook's distance was estimated to look for cases with undue influence. The regression analysis was also done with a bootstrap with 8000 runs to generate Bias-corrected accelerated 95%CI's for *b*. and an adjusted p for the correlations. For dependents with significant influence, the adjusted R^2 was calculated using Stein's formula.

Results

Satellite cells in healthy EOMs (Paper 1)

In EOMs of adult, healthy donors, Pax7-positive cells were quantified in the anterior, middle and posterior portion, as well as in the orbital and global layer of the middle and posterior portions. Please note that the anterior portion of the EOM, close to the tendinous insertion into the globe, lacks a discernable orbital layer. The number of Pax7-positive cells per myofiber was similar in the orbital and global layer in both the middle and posterior portions of the EOMs (Table 3, Paper 1). Pax7/F was significantly higher in the anterior portion of the EOMs of all subjects, compared to the middle and posterior portions. This higher value of Pax7-positive cells in the anterior part was not accompanied by any significant differences in mean CSA, N/F or myonuclear domain area. As N/F was similar in the middle and anterior portions, Pax7/N was also higher in the anterior portion. Interestingly, we found a slight, but significantly higher myonuclear domain area in the posterior portion of the EOMs. This difference was not reflected in a significant difference in N/F or mean CSA, but by comparing the overlapping confidence intervals of N/F and mean CSA between the middle and posterior portion, it seems that a lower N/F in the posterior portion contributes more to the higher myonuclear domain area than an increase in mean CSA along the middle-posterior axis.

Pax7-positive cells are found in non-traditional niches in the EOMs

Cells that were positive for NCAM and Pax7 (NCAM+/Pax7+) or just Pax7 (NCAM-/Pax7+) were also found in localizations that are not typical for SCs, (Figure 2, Paper 1). The percentage of myofiber-associated Pax7-positive cells varied from 56,5 to 89,3 percent along the length of the muscle and between donors with no statistical differences between the different portions. The percentage of interstitial Pax7-positive cells varied from 7,4 to 39,8 with most variation found between the individuals and not between different portions of the muscle. Other Pax7-positive cells that were in close apposition to non-myofiber structures such as blood vessels and nerve fascicles were few and varied between 0,0 and 7,1 per cent. Again, differences between individuals were more pronounced than differences between different portions of the EOM. For cells that were localized in the interstitium, it could be argued that connections with myofibers could be present just adjacent to our point of sectioning, and that the interstitial cells are an artefact of the cross-section preparation. To investigate this, confocal

images were generated from 30µm-sections, which was enough to visualize entire interstitial Pax7-positive cells. No quantitative investigation was undertaken because of laborious steps involved in imaging these cells, but several cells were found that were "truly" interstitial. Other cells were also found that superficially resembled interstitial cells, but where one end of the cell was attached via a thin, threadlike laminin-labeled membrane to a myofiber. Other cells seemed to form nucleus-wide appendages that branched off from existent myofibers that grew parallel to, but not in contact with the parent myofiber (except at the branching point).

Satellite cells in terminal ALS patients (Paper 2)

Gross morphology and NCAM labeling

As reported previously, EOMs from ALS patients displayed only mild morphological changes compared to the changes that were present in the limb muscle of the same patients. The most prevalent difference between the middle-aged or older controls and ALS patients was an increased myofiber size in some parts of the global layer in ALS patients. (Figure 1:e–h, Paper 2) The weak NCAM staining present in the cytoplasm of myofibers reported in paper 1 was also present in ALS patients. Very rarely, a small number of myofibers were present with a strong NCAM labeling, resembling regenerating fibers in the limb muscles. The biceps brachii muscles of aged controls displayed the typical cobblestone appearance normally found in limb muscles. In one 82-year old control, there were some signs of general atrophy and an increased number of angular myofibers. This is regularly found in biopsies of older human donors and becomes especially more prominent after the eighth decade of life [98]. Very few myofibers labeled for NCAM were found in the biceps of controls. In limb muscles of ALS patients, there were many signs of muscle denervation, such as grouped atrophy, hypertrophic myofibers with or without fiber splitting, angular fibers and increased connective tissue. The extent of changes varied between donors and between individual muscles of the same donor. The most severe changes were seen in muscles closer to the site of onset, i.e. lower limbs in lower limb onset patients, and upper limbs in bulbar and upper limb onset patients. In muscles far from the site of onset, the morphological changes were more moderate, but still noticeable compared to the biceps brachii muscles of controls. In most limb muscle samples, there were 10-15 myofibers strongly labeled for NCAM with a thickened basement membrane and, usually filled with numerous nuclei, suggesting ongoing repair. In one vastus lateralis muscle sample from ALS patient 12, a much higher number of NCAM-

labeled fibers was encountered, approximately 200 out of the 21000 myofibers in the whole cross-section.

Quiescent, proliferating and differentiating muscle progenitor cells in the EOMs of ALS patients

The number of Pax7-positive cells per myofiber was very similar in the middle portion of EOMs of ALS patients and age-matched controls ($p<0,743$). The ratio of interstitial Pax7-positive cells to the total number of Pax7-positive cells was also similar, but showing a possible trend that it might be lower in ALS patients ($p<0,080$). Pax7/N was significantly lower in ALS patients ($p<0,037$) but could not be correlated with an increase in N/F ($p<0,177$). There was a significant increase in mean CSA in the EOMs of ALS patients ($319\pm65\mu m^2$ versus 228 ± 43 μm^2, $p<0,019$) with no overt change in myonuclear domain area ($p<0,371$). A histogram displaying the pattern of CSA differences between ALS patients and controls is provided in figure 3 of paper 2.

MyoD and myogenin-labeled cells were generally rare in the middle portion of EOMs of ALS donors and controls. In controls, three and four MyoD labeled cells, respectively, were found in the whole muscle cross-sections. The densities were 0,28 and 0,47 nuclei per mm^2 of total myofiber area, respectively. Myogenin labeled cells were even fewer than MyoD labeled cells, but correlated well with the number of MyoD labeled nuclei found in the same subject. In the controls, no myogenin labeled nuclei were found in one sample, and only one was found in the other samples. In ALS EOMs, three samples contained no myogenin labeled nuclei, and two samples contained one (in SC position) and two (in subsarcolemmal position) myogenin labeled nuclei, respectively. Ki-67 labeled nuclei were categorized according to whether they were present in, or sharing basement membrane with, a myofiber as these labeled cells were considered more likely to represent replicating muscle progenitor cells. Other Ki-67 labeled nuclei were found in vessel walls, vessel lumens and connective tissue but were not considered to be of myogenic origin for density estimations. The density of myofiber-associated Ki-67 labeled nuclei was between 0,69-0,73 in controls and 0,0-0,21 in ALS patients.

Satellite cells and other myogenic progenitor cells in limb muscles of ALS patients

The number of SC/F did not differ between biceps brachii samples of ALS patients and controls ($0,054\pm0,024$ in ALS versus $0,037\pm0,020$ in controls).

Other estimates, such as mean CSA, SC/N, N/F and myonuclear domain (Table 4, Paper 2) were not significantly different between ALS patients and controls. The only estimate that showed any trend toward being different was SC/N, which was marginally higher in ALS patients than in controls (3,1±1,1% versus 1,9±0,5%, p<0,06). However, the proportion of total myofiber area differed significantly, with ALS patients displaying smaller propotional myofiber area than controls (73,0±5,4% versus 83,2±0,9%, p<0,006). In lower limb muscles, a large variation in all estimates was present. The number of SC/F was very high in the gastrocnemius muscle of the two donors with lower leg onset and slow progression (0,317 and 0,206, respectively). In the other donors, SC/F ranged from 0,052 to 0,108 in the gastrocnemius muscle.

MyoD labeled nuclei were rare but still present in most limb muscles analyzed. However, in one control and two ALS biceps brachii and one ALS vastus lateralis samples, a deviant labeling pattern was present. In these samples, a very weak to moderate granular labeling with the MyoD antibody was present in approximately half of all subsarcolemmal nuclei. Originally suspected to be an artefact, it became apparent that this labeling pattern was consistently present on repeated experiments of the same samples, did not change when new batches of the same primary antibody were tested and did not seem to be donor-specific, as this pattern was not present in more than one muscle from the same donor. For example, the donors with deviant MyoD labeling pattern in the biceps samples had normal MyoD labeling patterns in the vastus samples and vice versa. In addition, this labeling pattern was present in both donors with shorter and longer times to autopsy. Also, whereas MyoD labeling in the other samples tended to correlate well with the number of myogenin and Ki-67 labeled nuclei in those samples, the high numbers of weakly labeled MyoD myonuclei in the remaining samples was not accompanied by higher numbers of myogenin or Ki-67 labeled nuclei. This deviant labeling pattern, when present, made MyoD quantification unsatisfactorily arbitrary, since labeling levels in the myonuclei varied considerably. Therefore, no definite numbers of MyoD labeled nuclei were derived from these samples. We suspect that this labeling pattern may reflect another role of MyoD in muscle biology (please see discussion) and these four samples were therefore excluded in the calculation of MyoD-nuclei density.

The number of MyoD labeled nuclei ranged between 0-2 in control biceps, zero and 13 in ALS biceps brachii, 4-32 in ALS vastus lateralis and 1-19 in ALS gastrocnemius muscles. Translated into nuclei per mm^2 of total myofiber area, this translates 0,0 to 0,01/mm^2 MyoD nuclei in control biceps brachii, 0 to 1,27 nuclei/mm^2 in ALS biceps brachii, 0,21 to 0,84 nuclei/mm^2

in ALS vastus lateralis and 0,03 to 0,42 nuclei/mm² in gastrocnemius muscles. In ALS biceps brachii samples, most MyoD labeled nuclei were found in SC positions. The two MyoD nuclei found in the control biceps brachii muscles were found in myonuclear positions.

The number of myogenin labeled nuclei was generally lower than that of MyoD labeled nuclei, but tended to follow a similar pattern, that is, in the samples where there were more MyoD labeled nuclei, there were also more myogenin labeled nuclei. In control biceps, no myogenin labeled nuclei were found, despite the large total myofiber area (144−169 mm²) of some samples. In ALS biceps brachii muscles, five samples had no myogenin labeled nuclei, one sample had one labeled nucleus and one sample had three labeled nuclei (the same sample that had 13 MyoD labeled nuclei). In ALS vastus lateralis muscle, one sample lacked myogenin labeled nuclei and the remaining samples had 2-72 labeled nuclei. The sample with the very high number of myogenin labeled nuclei (72) was the vastus lateralis sample from donor 12 that had 32 MyoD labeled nuclei and a large number of regenerating myofibers strongly labeled for NCAM. In ALS gastrocnemius muscles, one sample lacked myogenin labeled nuclei and the remaining four had 3 to 6 myogenin labeled nuclei (Table 5, Paper 2).

As above for the EOMs, Ki-67 labeled nuclei were also frequently found in positions unlikely to be related to muscle progenitor cells in the limb muscle samples, and were therefore omitted from the estimation provided below. In control biceps brachii muscles, one sample was devoid of myofiber-associated Ki-67 labeled nuclei, two samples had one labeled nucleus each and one sample had five labeled nuclei. The resulting density was 0 to 0,06 nuclei per mm² of total myofiber area. In ALS biceps brachii, three samples were devoid of Ki-67 labeled nuclei, whereas the remaining had one to four labeled nuclei, translating into a Ki-67 density of 0 to 0,39 nuclei per mm² of total myofiber area. In ALS vastus lateralis, the number of labeled nuclei ranged from four to 45, with the higher number representing the aforementioned vastus sample with a high degree of regeneration. The density of labeled nuclei ranged from 0,12 to 1,18 nuclei per mm² of total myofiber area. In ALS gastrocnemius muscles, Ki-67 labeled nuclei ranged from zero to four, with densities per mm² of total myofiber area ranging from 0,0 to 0,11. Surprisingly, while muscle sections were labeled for both Pax7 and Ki-67, out of all samples stained for these markers, only one single nucleus were found (in donor 12) that was labeled for both Pax7 and Ki-67.

Motor endplate occupancy of NMJs in EOMs and limb muscles of transgenic of SOD1 mice (Paper 3)

The gross morphological changes present in the muscles of the transgenic mouse model G93A mirrored those earlier described in the ALS donor material. Namely, limb muscle specimens displayed severe grouped atrophy, central nuclei, scattered groups of hypertrophic myofibers, increase of connective tissue and fatty replacement, whereas the EOM specimens displayed only very mild signs of involvement with an apparent slight increase in fiber size variability (Figure 1 and 2, Paper 3)

In the course of method development, we found that longitudinal and cross-sectional approaches could both be safely used to characterize the innervation status of NMJs. However, given the extended shape of the postsynaptic part of the NMJ, cross-sectional orientations warranted an evaluation on four adjacent 8-μm sections to correctly identify complete denervation of a given NMJ. Longitudinal sections proved to be more efficient in the identification of denervated myofibers, as NMJs that apparently lacked the terminal axon on one such 8-μm section generally lacked the terminal axon on all subsequent, adjacent sections.

We found that the innervation ratio of NMJs was very high in EOMs of both G93A mice and controls (97,8±2,8% in G93A versus 98.6±2,2% NMJs innervated in Wt controls) whereas G93A mice had a significantly decreased innervation ratio in hind limbs compared to Wt littermates (70,9±10,8 in G93A% versus 97,2±3,4% in Wt controls).

After paper 3 was published, an additional statistical analysis has been conducted since non-difference is difficult to assess at a statistical level. To make a meaningful estimate of the similarity of innervation ratio between EOMs of wild-type and SOD1[G93A] mice, the maximum difference in a 95% bootstrapped Bias-corrected and accelerated confidence interval (4000 runs) was calculated. The maximum 95%CI difference of this bootstrap was 3,79%.

We also investigated the innervation of EOMs in three transgenic mice homozygous for SOD1[D90A] mutations and two of their wild-type littermates. Preliminary data showed no differences in the innervation status of the EOMs between transgenic mice and control littermates (mean innervation 100% in D90A mice versus 97,49% in controls). Due to unrelated breeding problems at the time of the study, we were unable to expand the groups of animals enough to include them in the original paper, but the data is provided here as additional support to the aforementioned results.

Loss of slow tonic myofibers in terminal ALS (Paper 4)

The proportion of myofibers co-labeled for MyHCsto and MyHCI was decreased in the global and orbital layers of the EOMs of ALS donors. Simultaneously, there were significantly higher numbers of myofibers labeled for MyHCI alone in the global layer of ALS donors, and a similar trend for MyHCI fibers in the orbital layer ($p < 0.053$). However, the higher proportion of MyHCI-only fibers in ALS patients did not balance the lower proportion of MyHCI+sto and therefore, the total proportion of fibers labeled for either slow MyHC was decreased (Figure 2, Paper 4) In both patients and controls, MyHCI-only fibers were significantly more frequent in the global layer than the orbital layer, and MyHCI+sto fibers were statistically more frequent in the orbital layer than the global layer in all groups except bulbar onset cases, where $p < 0.069$.

The labeling pattern of MyHCI+sto fibers differed between the EOM layers. In the orbital layer, myofibers labeled with the MyHCsto antibody showed a very strong labeling intensity, whereas the labeling intensity for the MyHCI antibody was more moderate. In the global layer, MyHCI labeling was very strong, whereas MyHCsto labeling was relatively weak. This labeling pattern was seen in all control samples, but in ALS donors, a minor proportion of myofibers (not quantified for methodological reasons, but estimated to less than 5%) in the orbital layer exhibited strong labeling for MyHCI and weaker labeling for MyHCsto, i.e. a labeling pattern similar to that of MyHCI+sto fibers in the global layer. The reverse (strong MyHCsto and moderate MyHCI in the global layer) was not seen in any sample.

The CSA of MyHCI+sto fibers was significantly smaller in the global layer than in the orbital layer of both ALS groups ($p < 0.024$ in bulbar onset cases and $p < 0.010$ in spinal onset cases), but not in controls ($p < 0.712$). In controls, MyHCI-only fibers were somewhat smaller, but not significantly so, than MyHCI+sto fibers in the orbital ($p < 0.055$) and global ($p < 0.055$) layers. In ALS patients, MyHCI-only fibers were significantly smaller than MyHCI+sto fibers in the orbital layer of both bulbar onset ($p < 0.049$) and spinal onset ($p < 0.014$) cases. In the global layer, MyHCI-only fibers were smaller than MyHCI+sto fibers in bulbar onset ($p < 0.024$), but not spinal onset ($p < 0.985$) cases. There were no significant differences in the CSA of MyHCI-only and MyHCI+sto fibers, between the separate groups of ALS patients.

Discussion

This thesis explored distinctive traits of EOM that may be of importance for their relative sparing in ALS. Since EOMs are fundamentally different from limb muscles in several regards, a number of hypotheses can be put forwards as to which of these differential characteristics may play a role for EOM sparing in ALS. Even though motor neuron loss is the major hallmark of ALS, several studies point to ALS being a systemic disease where other cells influence the disease course.

   We investigated SCs and other muscle progenitor cells in EOMs and limb muscles of ALS patients as these cells have been previously proposed to be involved in the unique response of the EOMs to disease and also reported to be affected in ALS [52,68,71,73,74]. Differences between EOMs and other skeletal muscles that may be essential for EOM sparing in ALS could also be located at the NMJ, either due to differences in the properties of the terminal axon or, alternatively, essential differences could derive from the properties of the myofibers of the EOMs and their ability to maintain the innervation or promote collateral innervation by other, less affected motor neurons. Therefore, we investigated the innervation of EOMs in general, by investigating the motor endplate occupancy in the SOD1[G93A] mouse model and the particular involvement of MyHCsto myofibers in human ALS donors, as they represent a myofiber type with several unique characteristics related to their innervation.

Myogenic progenitor cells in human EOMs (Paper 1)

The main findings of the first paper were: 1) Pax7-positive cells were not as abundant in the middle and posterior EOMs as previously described, but are relatively numerous in the anterior portion; 2) Pax7-positive cells of the EOMs were not only present in a SC position, but also frequently present in other niches and can even be found completely dissociated from myofibers in the loose interstitium between myofibers and 3) the myonuclear domains of EOM myofibers were very small compared to those of other muscles. A previous study on SCs, based on EOMs from four human donors reported that *"approximately 7% of the myofibers [are] associated with Pax7-positive satellite cells in human EOM"* [99] Given no measure of the variability between individual donors, it is difficult to assess how much deviation from 7% should be considered notably different. In paper 1 of this thesis, no donors exhibited Pax7/F ratios higher than 4% (0,040 in the non-converted ratio form used in the paper) in the middle and posterior portions, and the mean Pax7/F for these parts of the muscle were 0,028±0,005 and 0,028±0,007,

respectively. In the anterior portion, however, the mean Pax7/F was 0,076±0,022, much closer to the previously reported estimates [99].

The observation of Pax7/NCAM positive cells in niches normally not associated with SCs raises questions on their possible roles and origin. Some of these variant cell localizations have been noted previously in human studies on limb muscles, but not in such high numbers and not in a position completely detached from an adjacent myofiber [82,100]. One possibility is that those cells that are located in the interstitium have never been committed to the SC niche during the formation of the EOMs and therefore represent a pool of more immature progenitor cells. While data from paper 1 suggested that high SC numbers were not a general feature of the EOMs, but were rather restricted to the anterior portion, there is good experimental data that shows that at least some SCs of the EOM have a good proliferative capacity in vitro and in vivo, that exceeds that of limb muscles SCs [69]. Further studies will be needed to determine whether this superior proliferative capacity is a general phenotype of all myogenic progenitors in the EOMs, a phenotype related to the position along the length of the muscle or related to the interstitial Pax7-positive cells encountered along the whole length of the muscle.

The small myonuclear domains found in this study, despite being based on two-dimensional stereology, imply that the volume of cytoplasm surrounding each myonucleus is much smaller in EOMs than in other muscles. This could reflect the high metabolic rate of EOMs, with a higher need for protein turnover that mandates a higher density of nuclei. In limb muscles, type I fibers, having a higher continuous activity than type II fibers, also have higher numbers of myonuclei per fiber despite their generally smaller CSA, possibly to handle the higher protein turnover that comes with frequent activity [64]. Alternatively, or perhaps in parallel, there could be a physiological minimum number of myonuclei required in the original myofiber formation that leads to a surplus of myonuclei in myofibers that have not grown beyond a certain CSA, supported by data showing that whereas CSA of myofibers increase linearly throughout childhood, increases in N/F does not seem to appear before the age of 4 [101].

Satellite cells and myogenic progenitor cells in ALS (Paper 2)

The main findings of the second paper were: 1) the number of Pax7-positive cells per myofiber in the EOMs did not differ between age-matched controls and ALS patients; 2) in the biceps brachii muscle, the number of SCs per myofiber did not differ between ALS patients and controls; 3) EOM

myofibers as a whole, had a larger mean CSA in ALS patients than in controls; 4) in limb muscles of ALS patients, replicating and differentiating muscle progenitor cells, as shown by MyoD and myogenin antibody reactivity and further supported by Ki-67 labeling, were commonly encountered in positions indicative of a response to increased loads but could also be seen in regenerating fibers; 5) activation of SCs was rare in the absence of substantial hypertrophy and regenerating fibers, both in EOMs and limb muscles; 6) high numbers of SCs could be detected in gastrocnemius muscle samples of ALS patients with very long disease duration, but in all other muscles, a correlation between SC parameters and survival was absent and 7) there was a deviant MyoD labeling pattern in some biceps brachii and vastus lateralis muscle samples of controls and ALS patients that might be indicative of a broader role of MyoD in muscle homeostasis.

A previous study has quantified the presence of SCs in upper limbs of ALS patients [78]. Using electron microscopy, SC numbers were investigated in biopsies from five patients with approximately one year of disease duration. In comparison with controls, SC numbers did not differ between patients and controls, neither when analyzed in relation to myofiber numbers or the number of myonuclei. This study indicates a normal abundance of SC in early ALS. However, the type of ALS and rate of progression in the individual patients are not provided. Since the survival of one patient can differ several years or decades from another, one year after onset could indicate that a patient is in the early stage, as well as the terminal stage of the disease. Still, the study provided a paralysis grading on a four-level scale and indicated that at least two patients had some remaining upper limb function at the moment of biopsy. Therefore, the data can be interpreted to at least indicate the number of SCs in living ALS patients with some remaining survival time. Together with data from the current study, it appears likely that the abundance of SCs in the upper limb muscles does not differ from controls in either the symptomatic or terminal stages of ALS. Our study also showed that the numbers of muscle progenitor cells do not change dramatically in the EOMs of ALS patients in comparison to controls. The Pax7/F ratios were very similar in the EOMs of ALS patients and controls ($0{,}027\pm0{,}006$ versus $0{,}028\pm0{,}005$), whereas a significant decrease in Pax7/N was noted in the ALS patients. One possible explanation could be that a higher mean myonuclear content of ALS patients could result in a decreased ratio of Pax7/N. The increase of N/F in the EOMs of ALS patients was not significant, but the mean myofiber CSA of ALS patients was significantly larger. It has been previously recognized that as small myofibers in limb muscles grow beyond their postnatal size during childhood, this is usually accompanied by an increase in N/F and a decrease in SC/N [60]. Possibly,

similar correlations apply in the case of EOMs that grows beyond their normal myofiber CSA.

Earlier in vitro studies of human SCs from ALS patients suggest that the differentiating ability of proliferating SCs is diminished and that their ability to form myotubes is inhibited [73,74]. Based on these studies and studies in the SOD1[G93A] mouse model, it has been suggested that repeated rounds of activation, replication and regeneration eventually leads to senescence and a depletion of the SC pool [71,74]. If this was the case, we would expect the number of SCs and other muscle progenitor cells to decrease and that the ability of myofibers to be repaired and undergo hypertrophic growth in vivo would decrease, as the disease progressed. In limb muscles of ALS patients, activated SCs were readily encountered in fibers undergoing repair, as shown by MyoD, myogenin and Ki-67 labeled nuclei present within damaged myofibers with weakened or absent dystrophin labeling, but were even more prevalent in localizations where they were likely to contribute to myofiber growth, i.e. inside of the basement membrane or in subsarcolemmal positions in myofibers with an intact sarcolemma. Overall, the amount of differentiating SCs was low in EOM and biceps samples of both controls and patients.

The deviant MyoD labeling pattern found in some of the limb muscle samples was notably weaker, present primarily in myonuclei which normally only rarely displayed MyoD labeling, highly abundant (>500 nuclei per section) and did not remotely correlate with the number of myogenin and Ki-67 labeled nuclei of those samples. This deviant labeling pattern could be due to aberrant binding of the primary antibody to a shared epitope of a related or unrelated protein. However, MyoD regulation is complex [102] and general up-regulation of MyoD has been reported previously, both in response to denervation [103-105] and to loading [106,107]. These data are mostly derived from whole-muscle analysis with western blots [103,105] and/or qPCR [103,105-107], but some include immunostaining methods where MyoD was seen mainly in large groups of myonuclei [104,108]. Based on loading and denervation experimental studies, this increase in MyoD appears to very dynamic, with upregulation of MyoD appearing and disappearing in the course of hours in response to loading [102] or over weeks in response to denervation [109,110]. In our muscle samples, MyoD labeling in myonuclei appears to be a local phenomenon. Since the labeling reaction was also noted in one of the control biceps, most likely it cannot reflect denervation alone. Another possible explanation is that the reaction is a response to high loading of that particular muscle shortly before death, with or without the concomitant changes related to recent denervation.

During the analysis of sections labeled for Pax7, Ki-67 and laminin, simultaneously labeling of Pax7 and Ki-67 was noted only once, in a single nucleus, out of the seven EOMs and 21 limb muscles analyzed. As Pax7 has been shown to be present in active, replicating SCs [80], we would expect a considerable number of Pax7-positive cells to be co-labeled with Ki-67, at least in the lower limb muscle samples that exhibited clear signs of ongoing myofiber regeneration. Numerous Ki-67 labeled nuclei were found in regenerating myofibers, but none were co-labeled with Pax7, despite the concurrent presence of Pax7-positive cells in and in the vicinity of such myofibers. One study examining Wnt-signalling in SC activation [111], demonstrated Pax7/Ki-67 double-labeled cells in clinical biopsies of a young patient with limb girdle muscular atrophy, using the same antibodies and a similar protocol to ours [111]. The very low presence of double labeling in our material could indicate that this double-labeling pattern disappears relatively quickly after death, as no donors in our material were autopsied earlier than 14 hours post-mortem.

In our data, there was little indication that SC function decreased with increasing disease duration. This was best exemplified by patient 1 and 2, who both had lower leg onset of symptoms and long disease durations, over 11 and 26 years, respectively. Both patients were homozygous carriers for the well-known $SOD1^{D90A}$ mutation and their clinical profile corresponded well to the typical presentation for this type of mutation [5]. In patient 1, with the longest survival, there was very extensive hypertrophy (mean CSA = 8033 μm^2) coupled with an extensively expanded SC pool (SC/F = 0,32) and a high number of myonuclei per fiber (N/F=4,49) in the gastrocnemius muscle sample. Unfortunately, no upper limb specimens were available from this patient. However, samples taken from the gastrocnemius, vastus lateralis and biceps brachii muscles of the other $SOD1^{D90A}$ patient with >11 years of survival had similar, though less extreme changes. The mean CSA of the gastrocnemius muscle sample of this patient was still high (4594 μm^2), as was the SC number (SC/F=0,21). Even though disease duration and SC/F correlated in the 5 available gastrocnemius muscle samples, there was neither any positive nor negative correlation between SC/F or SC/N with survival in the biceps brachii or vastus lateralis muscle samples. Together, these observations suggest that SC function remains good enough to support extensive hypertrophy in ALS patients with very long disease duration, but that the size of the SC pool per se most likely has no association with survival in ALS.

Preserved motor endplate occupancy in the G93A mouse model (Paper 3)

The main findings of the third paper were: 1) the myofibers in the EOMs of G93A transgenic mice had a preserved innervation despite extensive denervation in their hind limb muscle fibers and 2) there were limited morphological changes observed in the EOM compared to limb muscles, akin to that previously reported in human donors [40]. This supports the notion that EOM sparing is not a human-specific feature of ALS, but could also be studied in mice. Other studies since then have reported similar results on EOM innervation of G93A mice [112] and further work from our group has demonstrated that human ALS patients also display a preserved NMJ innervation in EOMs in contrast to their limb muscles [113]. In an analysis of the sequential degeneration of the NMJ, the motor axon and finally, the loss of motor neurons in the SOD1[G93A] mouse model, retraction of the terminal axon from the motor endplate was reported to be an early change in the progression of ALS [84]. The preservation of NMJs in the EOMs of SOD1 transgenic mice and ALS patients suggest that this early deterioration of NMJs is somehow evaded in the EOMs and has prompted further investigations. Wnt signaling plays an important role in the branching of nerves, the formation of synapses, such as the NMJs and even during muscle regeneration [114]. Interestingly, a later study from our group showed that NMJs in the EOMs of terminal ALS patients and SOD1 mice maintain wnt signaling components that are lost in the NMJs of limb muscles [115]. Apart from generating muscular contractions, NMJs also serve as a site of retrograde transport of neurotrophic factors that provide important trophic stimuli to motor neurons [116]. In a very recent paper from our group we have shown that in the SOD1[G93A] mouse model, there is maintained labeling of three important neurotrophic factors (NT-4, GDNF and BDNF) at the NMJ of EOMs whereas they are decreased in the NMJs of limb muscles from terminal SOD1[G93A] mice [117].

While being a prerequisite for function, a preserved contact between the terminal motor axon and the motor endplate does not exclude the possibility of subtle changes that may affect the physiology of myofiber recruitment. For example, an electrophysiological study of motor units in the anconeus muscle in ALS shows that early fatigability of the NMJ is present at NMJs that have not yet been denervated [118]. Also, a more detailed characterization of the NMJs of EOMs in SOD1[G93A] mice at different disease stages revealed an increased proportion of endplates with a partial neurofilament labeling towards the end of their lifespan [112]. This suggests that subtle structural changes can occur at the NMJ if the disease progresses far enough. Laminin α2, one of the major proteins present in the basement membrane of nerves,

myofibers and NMJs, has been shown to decrease in the basement membranes of NMJs of the EOMs of terminal ALS patients and generally in the basement membranes of SOD1 mice models [119]. Concurrently, the NMJs of EOMs in terminal ALS patients have a maintained presence of laminin α4 in the basement membrane, whereas NMJs in limb muscles of terminal ALS patients have a much lower presence of laminin α4 than what is normally seen at the NMJs of healthy controls [119]. This implies that while some structural components of the NMJs are lost even in the EOMs, others are preserved in comparison to the changes that occur in limb muscles of ALS patients.

The sequential nature of the disease and the sparing of certain muscle groups is well known in ALS [2,13,40,44]. However, differential vulnerability is also present in different types of motor units within individual muscles afflicted by ALS [90,91,120]. It has been recognized that there is a sequential, predictable loss of motor units in limb muscles in ALS. The most vulnerable are fast-fatigable motor units, followed by fast-fatigue-resistant and finally slow-type motor units [90,91]. Given the high diversity of myofibers in the EOMs [33], further understanding of EOM sparing in ALS requires a more detailed description of the effects of ALS on the different types of myofibers present, and the types of motor units they represent. While myofibers and motor units in limb muscles are mainly segregated based on their contractile velocities and fatigability [121], EOM myofibers exhibit a remarkable diversity, depending on whether they are multiply innervated or not and also exhibit a continuum of metabolic and contractile profiles [18,33,122]. In addition, while limb myofibers normally contain one to two different MyHCs in their mature myofibers [123], EOM myofibers normally contain at least three isoforms [33]. Furthermore, individual myofibers may contain different MyHCs along their length [33].

Fast and slow myofibers in limb muscles exhibit characteristic NMJs in accordance to their electric input [124,125]. However, investigation of individual NMJs is very labor-intensive and consumes large amounts of material in the search for NMJ-rich areas of the muscle. One way to overcome this problem is to study the more accessible MyHC content of EOM myofibers since MyHC expression, while being complex in EOMs [33], still serves as an indicator of the type of motor unit it represents [27]. Therefore, the final paper of this thesis was an attempt to start dissecting the involvement of different fiber types in ALS and focused on one of the most characteristic types of myofiber present in the EOMs – the multiply innervated fibers containing MyHC slow tonic and MyHCI.

Loss of slow tonic myofibers in terminal ALS (Paper 4)

The main findings of the fourth paper were: 1) MyHCI+sto fibers were fewer in the global layer and orbital layer of EOMs in ALS patients; 2) MyHCI-only fibers were somewhat more abundant in the global layer of ALS patients, and possibly in the orbital layer too; 3) a possible, but not certain, atrophy of MyHCI+sto fibers was present in the global layer of ALS patients and 4) a substantial correlation between age of death and loss of MyHCI+sto fibers was present in the global layer of bulbar onset patients, but neither in spinal onset patients nor in controls.

Loss of double-labeled MyHCI+sto fibers in the medial rectus with a small, incomplete increase in the proportion of MyHCI-only fibers might indicate that these MyHCs are lost sequentially in the myofiber, with MyHCsto being lost first and later followed by a loss of MyHCI. Loss of MyHC isoforms could indicate a loss of motor neuron connectivity and reinnervation by another type of motor unit, as is normally found in chronic denervation [126]. Alternatively, the shift in MyHC isoform could indicate that the neuronal activity of the MIF-innervating motor neurons has changed, thus producing a shift in MyHC isoform content due to a different electrical input. A third possible explanation could be that ALS-related changes taking place in the MyHCI+sto myofibers decreased the epitope availability of these MyHCs recognized by the antibodies used. It has been previously shown in the human EOMs and limb muscles that different antibodies against MyHCI bind differently to myofibers depending on their developmental status and studies in mice have implied that this depends on changing post-translational modifications of MyHCI during the maturation process of the myofiber [127,128]. In murine limb muscles, the innervation of slow myofibers appears to play a pivotal role in whether the maturation-related epitope will be available or not [129]. In our study, we used the A4.951 monoclonal antibody that is suggested to primarily label mature, innervated slow myofibers [129]. It is therefore possible that some myofibers in the EOMs of our donors would have been detectable with the use of another antibody against MyHCI, and further work will be needed to discern whether such a discrepancy is present in the slow myofibers of EOMs from ALS donors. Regardless of whether this change in MyHC isoform content is due to an actual loss of motor neurons, a change in electric activity or a change in the post-translational modifications of these MyHC isoforms, it suggests that slow-type motor neurons in the oculomotor nuclei may somehow be affected in terminal ALS patients. This is an interesting contrast to the pattern of neuronal loss previously reported in limb muscles, where slow-type motor neurons survive the longest [90,91]. Possibly, the myofibers that once contained MyHCsto and MyHCI (as detectable by the antibodies used) but then subsequently lost these MyHC

isoforms are still present in the EOMs, given that the EOMs of ALS patients did not contain an increased population of atrophic and presumably denervated myofibers in contrast to the biceps brachii muscles of ALS patients (compare Figure 3 and 7, Paper 2). This maintained pool of innervated myofibers is also supported by the preserved axonal contact in the EOMs of SOD1[G93A] mice reported in paper 3, which has later been confirmed in terminal ALS patients [113]. Investigating the actual fate of the MIF-innervating motor neurons, whether they are lost in ALS or not, will require studies of the oculomotor nucleus, where MIF-innervating motor neurons can be found in their own niche and express a different set of surface markers compared to SIF-innervating motor neurons [94-96]. However, such investigations have to take into account that MIFs display further differences in MyHC composition and electrophysiological properties in the orbital and global layers [33,122]. For examples, orbital MIFs more commonly co-express α-cardiac MyHC than global layer MIFs [33], and electrophysiologically, the NMJs in the midbelly region of orbital layer MIFs are able to generate action potentials, whereas global layer MIFs only contain the more primitive, non-spiking en-grappe NMJ type [122]. Notably, the more consistent loss of global layer MyHCI+sto myofibers, in paper 4 coupled with a trend towards smaller CSA in these myofibers, suggested that these MIFs were more affected in ALS than their orbital layer counterparts. This indicates that different subgroups of MIF-innervating motor neurons in the oculomotor nucleus might be differentially affected in ALS. Furthermore, while the fate of SIFs of the EOMs have not been investigated in this thesis, investigating the motor neurons innervating these SIFs could also be of importance as they constitute at least two classes of motor neurons, the so-called type I_A and type I_B [26], which possibly also could show different degrees of involvement in ALS.

Age-related loss of neurons is not a global phenomenon in the CNS. While age-related loss of grey matter has been widely documented in many regions, such as the hippocampus, frontal lobe and parietal lobe [130], most nuclei in the brainstem show no age-related loss of neurons at all [131-134]. The oculomotor nucleus, innervating the medial rectus, unlike the trochlear and abducens nuclei, has not been investigated in humans, but has been shown to maintain the same number of neurons over the lifespan in mice [135]. This is in line with our findings that MyHCI+sto fiber proportions did not correlate with the age of our subjects and that our mean proportions were very similar to those reported in an earlier study on MyHCI fibers that was based on a younger cohort (mean age: 37,5 versus 66,0 years in paper 4)[33].

Interestingly, the results of paper 4 suggested a significant, age-related decline in MyHCI+sto fibers in ALS patients with bulbar onset. Initially

when MyHCI+sto loss was revealed in the statistical analysis, disease duration was suspected to be a determinant of MyHCI+sto. The hypothesis was that with a protracted disease course, the relative sparing of EOMs would become less and less apparent, especially in bulbar onset cases where more involvement of the brainstem could be expected. Unexpectedly, disease duration was not remotely associated (p<0,293 for bulbar cases and p<0,813 in spinal cases) with MyHCI+sto proportions in the global layer in our patient cohort. Based on the regression slopes and assumption that the loss of MyHCI+sto is linear, the loss of MyHCI+sto fibers would be the equivalent of 1 to 4 percent of the total number of fibers per decade. In comparison with the loss of MyHCI+sto fibers present in the EOM samples, this would suggest a loss of MyHCI+sto fibers that pre-dated the disease onset by years or even decades. Investigating the fate of the motor neurons supplying multiply innervated fibers in the EOMs may give further indications on how ALS spreads through the CNS.

Importantly, the findings of paper 4 suggest that whereas EOMs as a whole are relatively spared in ALS, MyHCI+sto fibers are not. This warrants further studies of how the remaining myofiber types and their corresponding motor neurons, despite high metabolic demand and intense neuronal activity, are able to remain functional and to maintain their NMJs, even in terminal ALS.

Conclusions

In summary, the answers to the questions stated under the aims of the thesis are:

- The content of Pax7-positive, which make up most of the SCs and other muscle progenitor cells of human EOMs, was considerably lower in the middle and posterior parts of the muscle than what has been previously reported.

- Pax7 cells were not evenly distributed along the length of the EOMs, being approximately twice as many in the anterior portion of the muscle as in the other parts of the muscle.

- The ratio of Pax7 cells per myofiber was similar in the EOMs of terminal ALS patients and controls. However, there was a lower ratio of Pax7 cells per myonuclei in EOMs of ALS donors.

- SCs were as abundant in the biceps muscles of ALS patients as in aged controls.

- Muscle progenitor cells at different stages of replication and differentiation were found in both EOMs and limb muscles, but were usually sparse in EOMs and biceps of controls and ALS patients. In lower limb muscles of ALS patients, replicating and differentiating muscle progenitor cells were more common, but did not differ in abundance between patients with short or long survival.

- There was no indication of depletion of SCs in terminal ALS patients. In addition, two cases with SOD1^{D90A} mutations indicated that very long survival was rather associated with a larger, but still efficient, SC pool.

- Unlike limb muscles, there were preserved contacts between the terminal motor axons and the motor endplates in the EOMs of the SOD1^{G93A} mouse model and possibly also in the SOD1^{D90A} mouse model.

- In the EOMs of terminal ALS patients, there was a notable loss of myofibers containing both MyHC slow tonic and MyHC slow twitch.

- This loss was not associated with disease survival length, but in bulbar onset patients, there was a correlation between loss of MyHC slow tonic and aging.

In conclusion, our data suggested that SCs play a minor role in the progression of ALS in general and in the sparing of the EOMs in particular. The generally preserved innervation in the EOMs of G93A mice may reflect distinct intrinsic properties relevant for sparing of the oculomotor system. Even though the EOMs are relatively spared in ALS, MyHC slow tonic myofibers were selectively affected and this may reflect differences in innervation, as these fibers are multiply innervated.

Acknowledgements

I have had the great privilege of working alongside numerous skilled and friendly colleagues during the years leading up to this thesis. I am very grateful for being part of the warm working environment at Integrative Medical Biology and want to express a heartily thanks to every colleague I have engaged with during these years. Some people deserve a distinct mark of gratitude and those are accounted for below.

My first thanks goes to my main supervisor, Professor Fatima Pedrosa Domellöf. It was an unexpected but wonderful thing to be picked up as a simple carpenter's son and put into the exotic and peculiar world of research. You opened a really big door for me. To be given the opportunity to do research is a debt that cannot be repaid, only passed on. Later on, when I became a PhD student, you showed great insight again by giving me loose reins. I have always learned the most when my mind moved freely, and it shows courage on your part to let me run with my ideas (and your research grants) like I have. Finally, you have done me a great favor by persistently tutoring me on how to put those ideas down in writing. A great idea is worth nothing if no one else understands it.

My next thanks goes to my co-supervisor, Doctor Mona Lindström. A good scientist knows not only how to push forward, but also how to take a step back, observe your data from the outside and ask those important questions like: "Can I trust my results? Could it mean something else?" Results should always be scrutinized, regardless whether you like them or not, and you have taught me the healthy skepticism that every experimenter should carry with them. Also, you always demonstrated how to carry a cool head on you shoulders, right above a warm heart.

Thanks goes also to co-supervisor Professor Thomas Brännström, who happily shared his thoughts on the very important *other* half of the neuromuscular system. You also welcomed me into the most important room for this thesis, the autopsy room. Every meeting in that room was tinged with sorrow for the human life that had been lost, mixed with the cautious hope that our work could lead to a better future. You showed me that a Pathologist is no less a physician to his patients than any other specialist.

A special thanks goes to Professor Peter Andersen, who is very much the heart and soul of the ALS research consortium. In the end, it is all about the patients, their families, and their right to survival, I will not forget that.

Thanks also to Margaretha Enerstedt for giving me the first, essential lessons in laboratory work and Anna-Karin Olofsson for giving me the extended course.

Colleagues aside, this journey would have been much more difficult without the support of friends and family.

Thanks to my parents, Agneta and Björn, for creating the environment for a budding researcher since the very first day. Thanks also to my siblings, Cajsa and Karl-Johan, for excellent technical assistance in my first scientific investigations on the playground. You are the best siblings a brother can possibly have.

Thanks to Kent and Barbro, wonderful grandparents that always believed in me, allowed me to run amok with experiments in their kitchen and are very forgiving that I don't show up for coffee as often as I'd wish.

Greta Sonnsjö, I really wish you were still here...

Linus Tjust, my son, I watched you as your upper motor neurons formed synapses with you spinal motor neurons during the writing of this book. It was a wonder to behold. If action potentials were rays of light, I'm sure yours would be the most beautiful in the world.

Finally,
Thanks to my wonderful, resolute and brilliant wife, whom without I would be helplessly lost – Jasmine

When I try my best, but I don't succeed.
When I get what I want, but not what I need.

You fix me.

References

1.   Charcot, J.M. & Joffroy, A. Deux cas d'atrophie musculaire progressive avec lesion de la subsance grise et des daisceaux anterolateraux de la moelle epiniere. *Arch. Physiol. Neurol. Pathol.*, 744 (1869).

2.   Lawyer, T., Jr. & Netsky, M.G. Amyotrophic lateral sclerosis. *AMA Arch Neurol Psychiatry* 69, 171-192 (1953).

3.   Zarei, S.*, et al.* A comprehensive review of amyotrophic lateral sclerosis. *Surgical neurology international* 6, 171 (2015).

4.   Miller, R.G., Mitchell, J.D. & Moore, D.H. Riluzole for amyotrophic lateral sclerosis (ALS)/motor neuron disease (MND). *Cochrane Database Syst Rev*, Cd001447 (2012).

5.   Andersen, P.M. & Al-Chalabi, A. Clinical genetics of amyotrophic lateral sclerosis: what do we really know? *Nature reviews. Neurology* 7, 603-615 (2011).

6.   Rosen, D.R. Mutations in Cu/Zn superoxide dismutase gene are associated with familial amyotrophic lateral sclerosis. *Nature* 364, 362 (1993).

7.   McCord, J.M. & Fridovich, I. Superoxide dismutase. An enzymic function for erythrocuprein (hemocuprein). *J Biol Chem* 244, 6049-6055 (1969).

8.   Renton, A.E.*, et al.* A hexanucleotide repeat expansion in C9ORF72 is the cause of chromosome 9p21-linked ALS-FTD. *Neuron* 72, 257-268 (2011).

9.   Gurney, M.E.*, et al.* Motor neuron degeneration in mice that express a human Cu,Zn superoxide dismutase mutation. *Science* 264, 1772-1775 (1994).

10.   Olivan, S.*, et al.* Comparative study of behavioural tests in the SOD1G93A mouse model of amyotrophic lateral sclerosis. *Experimental animals / Japanese Association for Laboratory Animal Science* 64, 147-153 (2015).

11.   Zang, D.W. & Cheema, S.S. Degeneration of corticospinal and bulbospinal systems in the superoxide dismutase 1(G93A G1H) transgenic mouse model of familial amyotrophic lateral sclerosis. *Neurosci Lett* 332, 99-102 (2002).

12.   Okamoto, K.*, et al.* Oculomotor nuclear pathology in amyotrophic lateral sclerosis. *Acta Neuropathol* 85, 458-462 (1993).

13.   Mannen, T., Iwata, M., Toyokura, Y. & Nagashima, K. Preservation of a certain motoneurone group of the sacral cord in amyotrophic lateral sclerosis: its clinical significance. *J Neurol Neurosurg Psychiatry* 40, 464-469 (1977).

14. Sobue, G.*, et al.* Spinal and cranial motor nerve roots in amyotrophic lateral sclerosis and X-linked recessive bulbospinal muscular atrophy: morphometric and teased-fiber study. *Acta Neuropathol* 55, 227-235 (1981).

15. Takahashi, H., Oyanagi, K. & Ikuta, F. The intermediolateral nucleus in sporadic amyotrophic lateral sclerosis. *Acta Neuropathol* 86, 190-192 (1993).

16. Osorio, J. & Retaux, S. The lamprey in evolutionary studies. *Development genes and evolution* 218, 221-235 (2008).

17. Spencer, R.F. & Porter, J.D. Biological organization of the extraocular muscles. *Prog Brain Res* 151, 43-80 (2006).

18. Asmussen, G., Punkt, K., Bartsch, B. & Soukup, T. Specific metabolic properties of rat oculorotatory extraocular muscles can be linked to their low force requirements. *Invest Ophthalmol Vis Sci* 49, 4865-4871 (2008).

19. Wooten, G.F. & Reis, D.J. Blood flow in extraocular muscle of cat. *Arch Neurol* 26, 350-352 (1972).

20. Kjellgren, D., Thornell, L.E., Virtanen, I. & Pedrosa-Domellof, F. Laminin isoforms in human extraocular muscles. *Invest Ophthalmol Vis Sci* 45, 4233-4239 (2004).

21. Goldberg, S.J. & Shall, M.S. Motor units of extraocular muscles: recent findings. *Prog Brain Res* 123, 221-232 (1999).

22. Gueritaud, J.P., Horcholle-Bossavit, G., Jami, L., Thiesson, D. & Tyc-Dumont, S. Resistance to glycogen depletion of motor units in the cat rectus lateralis muscle. *Experimental brain research* 60, 542-550 (1985).

23. Floeter, M.K. Strucutre and function of muscle fibers and motor units. in *Disorders of Voluntary Muscle* (ed. Karpati, G.) (Cambridge University Press, 2010).

24. Dietert, S.E. The demonstration of different types of muscle fibers in human extraocular muscle fibers in human extraocular muscle by electron microscopy and cholinesterase staining. *Invest Ophthalmol* 4, 51-63 (1965).

25. Hess, A. The structure of slow and fast extrafusal muscle fibers in the extraocular muscles and their nerve endings in guinea pigs. *Journal of cellular and comparative physiology* 58, 63-79 (1961).

26. Nieto-Gonzalez, J.L., Carrascal, L., Nunez-Abades, P. & Torres, B. Phasic and tonic firing properties in rat oculomotor nucleus motoneurons, studied in vitro. *Eur J Neurosci* 25, 2682-2696 (2007).

27. Schiaffino, S. & Reggiani, C. Fiber types in mammalian skeletal muscles. *Physiological reviews* 91, 1447-1531 (2011).

28. Schiaffino, S., Rossi, A.C., Smerdu, V., Leinwand, L.A. & Reggiani, C. Developmental myosins: expression patterns and functional significance. *Skeletal muscle* 5, 22 (2015).

29. Hoh, J.F., Hughes, S., Hale, P.T. & Fitzsimons, R.B. Immunocytochemical and electrophoretic analyses of changes in myosin gene expression in cat limb fast and slow muscles during postnatal development. *Journal of muscle research and cell motility* 9, 30-47 (1988).

30. Mascarello, F., Toniolo, L., Cancellara, P., Reggiani, C. & Maccatrozzo, L. Expression and identification of 10 sarcomeric MyHC isoforms in human skeletal muscles of different embryological origin. Diversity and similarity in mammalian species. *Annals of anatomy = Anatomischer Anzeiger : official organ of the Anatomische Gesellschaft* 207, 9-20 (2016).

31. Bormioli, S.P., Torresan, P., Sartore, S., Moschini, G.B. & Schiaffino, S. Immunohistochemical identification of slow-tonic fibers in human extrinsic eye muscles. *Invest Ophthalmol Vis Sci* 18, 303-306 (1979).

32. Sartore, S.*, et al.* Fibre types in extraocular muscles: a new myosin isoform in the fast fibres. *Journal of muscle research and cell motility* 8, 161-172 (1987).

33. Kjellgren, D., Thornell, L.E., Andersen, J. & Pedrosa-Domellof, F. Myosin heavy chain isoforms in human extraocular muscles. *Invest Ophthalmol Vis Sci* 44, 1419-1425 (2003).

34. McLoon, L.K., Park, H.N., Kim, J.H., Pedrosa-Domellof, F. & Thompson, L.V. A continuum of myofibers in adult rabbit extraocular muscle: force, shortening velocity, and patterns of myosin heavy chain colocalization. *Journal of applied physiology (Bethesda, Md. : 1985)* 111, 1178-1189 (2011).

35. Pedrosa Domellof, F. Extraocular Muscle Involvement in Disease. *Reference Module in Neuroscience and Biobehavioral Psychology* In press(2017).

36. Kaminski, H.J., al-Hakim, M., Leigh, R.J., Katirji, M.B. & Ruff, R.L. Extraocular muscles are spared in advanced Duchenne dystrophy. *Annals of neurology* 32, 586-588 (1992).

37. Porter, J.D. & Karathanasis, P. Extraocular muscle in merosin-deficient muscular dystrophy: cation homeostasis is maintained but is not mechanistic in muscle sparing. *Cell Tissue Res* 292, 495-501 (1998).

38. Nystrom, A., Holmblad, J., Pedrosa-Domellof, F., Sasaki, T. & Durbeej, M. Extraocular muscle is spared upon complete laminin alpha2 chain deficiency: comparative expression of laminin and integrin isoforms. *Matrix biology : journal of the International Society for Matrix Biology* 25, 382-385 (2006).

39. Cohen, B. & Caroscio, J. Eye movements in amyotrophic lateral sclerosis. *Journal of neural transmission. Supplementum* 19, 305-315 (1983).

40. Ahmadi, M., *et al.* Human extraocular muscles in ALS. *Invest Ophthalmol Vis Sci* 51, 3494-3501 (2010).

41. Liu, J.X., Willison, H.J. & Pedrosa-Domellof, F. Immunolocalization of GQ1b and related gangliosides in human extraocular neuromuscular junctions and muscle spindles. *Invest Ophthalmol Vis Sci* 50, 3226-3232 (2009).

42. Fischer, M.D., *et al.* Definition of the unique human extraocular muscle allotype by expression profiling. *Physiol Genomics* 22, 283-291 (2005).

43. Ketterer, C., Zeiger, U., Budak, M.T., Rubinstein, N.A. & Khurana, T.S. Identification of the neuromuscular junction transcriptome of extraocular muscle by laser capture microdissection. *Invest Ophthalmol Vis Sci* 51, 4589-4599 (2010).

44. Walsh, F.B. & Hyot, A.B. Heredofamilial and degenerative diseases. in *Clinical Neuro-opthalmology*, Vol. 1 (eds. Walsh, F.B. & Hyot, A.B.) 936-938 (Williams & Wilkins Co, Baltimore, 1969).

45. Harvey, D.G., Torack, R.M. & Rosenbaum, H.E. Amyotrophic lateral sclerosis with ophthalmoplegia. A clinicopathologic study. *Arch Neurol* 36, 615-617 (1979).

46. Mizutani, T., *et al.* Development of ophthalmoplegia in amyotrophic lateral sclerosis during long-term use of respirators. *J Neurol Sci* 99, 311-319 (1990).

47. Hayashi, H. & Kato, S. Total manifestations of amyotrophic lateral sclerosis. ALS in the totally locked-in state. *J Neurol Sci* 93, 19-35 (1989).

48. Mizutani, T., *et al.* Amyotrophic lateral sclerosis with ophthalmoplegia and multisystem degeneration in patients on long-term use of respirators. *Acta Neuropathol* 84, 372-377 (1992).

49. Ohki, M., *et al.* Ocular abnormalities in amyotrophic lateral sclerosis. *Acta Otolaryngol Suppl* 511, 138-142 (1994).

50. Palmowski, A., *et al.* Eye movement in amyotrophic lateral sclerosis: a longitudinal study. *Ger J Ophthalmol* 4, 355-362 (1995).

51. McLoon, L.K. & Wirtschafter, J. Activated satellite cells are present in uninjured extraocular muscles of mature mice. *Transactions of the American Ophthalmological Society* 100, 119-123; discussion 123-114 (2002).

52. Kallestad, K.M., *et al.* Sparing of extraocular muscle in aging and muscular dystrophies: a myogenic precursor cell hypothesis. *Experimental cell research* 317, 873-885 (2011).

53. Mauro, A. Satellite cell of skeletal muscle fibers. *The Journal of biophysical and biochemical cytology* 9, 493-495 (1961).

54.   Relaix, F. & Zammit, P.S. Satellite cells are essential for skeletal muscle regeneration: the cell on the edge returns centre stage. *Development* 139, 2845-2856 (2012).

55.   Dreyer, H.C., Blanco, C.E., Sattler, F.R., Schroeder, E.T. & Wiswell, R.A. Satellite cell numbers in young and older men 24 hours after eccentric exercise. *Muscle Nerve* 33, 242-253 (2006).

56.   Lepper, C., Partridge, T.A. & Fan, C.M. An absolute requirement for Pax7-positive satellite cells in acute injury-induced skeletal muscle regeneration. *Development* 138, 3639-3646 (2011).

57.   Sambasivan, R.*, et al.* Pax7-expressing satellite cells are indispensable for adult skeletal muscle regeneration. *Development* 138, 3647-3656 (2011).

58.   Buckingham, M.*, et al.* Myogenic progenitor cells in the mouse embryo are marked by the expression of Pax3/7 genes that regulate their survival and myogenic potential. *Anatomy and embryology* 211 Suppl 1, 51-56 (2006).

59.   Wood, W.M., Etemad, S., Yamamoto, M. & Goldhamer, D.J. MyoD-expressing progenitors are essential for skeletal myogenesis and satellite cell development. *Developmental biology* 384, 114-127 (2013).

60.   Verdijk, L.B.*, et al.* Satellite cells in human skeletal muscle; from birth to old age. *Age (Dordrecht, Netherlands)* 36, 545-547 (2014).

61.   Kadi, F., Charifi, N., Denis, C. & Lexell, J. Satellite cells and myonuclei in young and elderly women and men. *Muscle Nerve* 29, 120-127 (2004).

62.   Verney, J.*, et al.* Effects of combined lower body endurance and upper body resistance training on the satellite cell pool in elderly subjects. *Muscle Nerve* 38, 1147-1154 (2008).

63.   Schmalbruch, H. & Hellhammer, U. The number of nuclei in adult rat muscles with special reference to satellite cells. *The Anatomical record* 189, 169-175 (1977).

64.   Verdijk, L.B.*, et al.* Satellite cell content is specifically reduced in type II skeletal muscle fibers in the elderly. *Am J Physiol Endocrinol Metab* 292, E151-157 (2007).

65.   Verdijk, L.B.*, et al.* Skeletal muscle hypertrophy following resistance training is accompanied by a fiber type-specific increase in satellite cell content in elderly men. *The journals of gerontology. Series A, Biological sciences and medical sciences* 64, 332-339 (2009).

66.   Fry, C.S.*, et al.* Fibre type-specific satellite cell response to aerobic training in sedentary adults. *The Journal of physiology* 592, 2625-2635 (2014).

67.   McLoon, L.K. & Wirtschafter, J.D. Continuous myonuclear addition to single extraocular myofibers in uninjured adult rabbits. *Muscle Nerve* 25, 348-358 (2002).

68. McLoon, L.K., Rowe, J., Wirtschafter, J. & McCormick, K.M. Continuous myofiber remodeling in uninjured extraocular myofibers: myonuclear turnover and evidence for apoptosis. *Muscle Nerve* 29, 707-715 (2004).

69. Stuelsatz, P.*, et al.* Extraocular muscle satellite cells are high performance myo-engines retaining efficient regenerative capacity in dystrophin deficiency. *Developmental biology* 397, 31-44 (2015).

70. Manzano, R.*, et al.* Quantity and activation of myofiber-associated satellite cells in a mouse model of amyotrophic lateral sclerosis. *Stem cell reviews* 8, 279-287 (2012).

71. Manzano, R.*, et al.* Altered in vitro proliferation of mouse SOD1-G93A skeletal muscle satellite cells. *Neurodegener Dis* 11, 153-164 (2013).

72. Manzano, R.*, et al.* Altered expression of myogenic regulatory factors in the mouse model of amyotrophic lateral sclerosis. *Neurodegener Dis* 8, 386-396 (2011).

73. Pradat, P.F.*, et al.* Abnormalities of satellite cells function in amyotrophic lateral sclerosis. *Amyotroph Lateral Scler* 12, 264-271 (2011).

74. Scaramozza, A.*, et al.* Skeletal Muscle Satellite Cells in Amyotrophic Lateral Sclerosis. *Ultrastructural pathology*, 1-8 (2014).

75. Dobrowolny, G.*, et al.* Skeletal muscle is a primary target of SOD1G93A-mediated toxicity. *Cell Metab* 8, 425-436 (2008).

76. Wong, M. & Martin, L.J. Skeletal muscle-restricted expression of human SOD1 causes motor neuron degeneration in transgenic mice. *Hum Mol Genet* 19, 2284-2302 (2010).

77. Liu, W., Wei-LaPierre, L., Klose, A., Dirksen, R.T. & Chakkalakal, J.V. Inducible depletion of adult skeletal muscle stem cells impairs the regeneration of neuromuscular junctions. *eLife* 4(2015).

78. Ishimoto, S., Goto, I., Ohta, M. & Kuroiwa, Y. A quantitative study of the muscle satellite cells in various neuromuscular disorders. *J Neurol Sci* 62, 303-314 (1983).

79. Illa, I., Leon-Monzon, M. & Dalakas, M.C. Regenerating and denervated human muscle fibers and satellite cells express neural cell adhesion molecule recognized by monoclonal antibodies to natural killer cells. *Annals of neurology* 31, 46-52 (1992).

80. Seale, P.*, et al.* Pax7 is required for the specification of myogenic satellite cells. *Cell* 102, 777-786 (2000).

81. Oustanina, S., Hause, G. & Braun, T. Pax7 directs postnatal renewal and propagation of myogenic satellite cells but not their specification. *EMBO J* 23, 3430-3439 (2004).

82. Lindstrom, M. & Thornell, L.E. New multiple labelling method for improved satellite cell identification in human muscle: application to a cohort of power-lifters and sedentary men. *Histochemistry and cell biology* 132, 141-157 (2009).

83. Lindstrom, M., Pedrosa-Domellof, F. & Thornell, L.E. Satellite cell heterogeneity with respect to expression of MyoD, myogenin, Dlk1 and c-Met in human skeletal muscle: application to a cohort of power lifters and sedentary men. *Histochemistry and cell biology* 134, 371-385 (2010).

84. Fischer, L.R.*, et al.* Amyotrophic lateral sclerosis is a distal axonopathy: evidence in mice and man. *Exp Neurol* 185, 232-240 (2004).

85. Fischer, L.R. & Glass, J.D. Axonal degeneration in motor neuron disease. *Neurodegener Dis* 4, 431-442 (2007).

86. Gould, T.W.*, et al.* Complete dissociation of motor neuron death from motor dysfunction by Bax deletion in a mouse model of ALS. *J Neurosci* 26, 8774-8786 (2006).

87. Raimondi, A.*, et al.* Cell culture models to investigate the selective vulnerability of motoneuronal mitochondria to familial ALS-linked G93ASOD1. *Eur J Neurosci* 24, 387-399 (2006).

88. Dupuis, L.*, et al.* Up-regulation of mitochondrial uncoupling protein 3 reveals an early muscular metabolic defect in amyotrophic lateral sclerosis. *FASEB J* 17, 2091-2093 (2003).

89. Dupuis, L.*, et al.* Muscle mitochondrial uncoupling dismantles neuromuscular junction and triggers distal degeneration of motor neurons. *PLoS One* 4, e5390 (2009).

90. Frey, D.*, et al.* Early and selective loss of neuromuscular synapse subtypes with low sprouting competence in motoneuron diseases. *J Neurosci* 20, 2534-2542 (2000).

91. Hegedus, J., Putman, C.T., Tyreman, N. & Gordon, T. Preferential motor unit loss in the SOD1 G93A transgenic mouse model of amyotrophic lateral sclerosis. *The Journal of physiology* 586, 3337-3351 (2008).

92. Padykula, H.A. & Gauthier, G.F. The ultrastructure of the neuromuscular junctions of mammalian red, white, and intermediate skeletal muscle fibers. *J Cell Biol* 46, 27-41 (1970).

93. Pun, S., Santos, A.F., Saxena, S., Xu, L. & Caroni, P. Selective vulnerability and pruning of phasic motoneuron axons in motoneuron disease alleviated by CNTF. *Nat Neurosci* 9, 408-419 (2006).

94. Eberhorn, A.C., Ardeleanu, P., Buttner-Ennever, J.A. & Horn, A.K. Histochemical differences between motoneurons supplying multiply and singly innervated extraocular muscle fibers. *The Journal of comparative neurology* 491, 352-366 (2005).

95. Eberhorn, A.C., Buttner-Ennever, J.A. & Horn, A.K. Identification of motoneurons supplying multiply- or singly-innervated extraocular muscle fibers in the rat. *Neuroscience* 137, 891-903 (2006).

96. Erichsen, J.T., Wright, N.F. & May, P.J. Morphology and ultrastructure of medial rectus subgroup motoneurons in the macaque monkey. *The Journal of comparative neurology* 522, 626-641 (2014).

97. Gundersen, H.J.*, et al.* Some new, simple and efficient stereological methods and their use in pathological research and diagnosis. *APMIS : acta pathologica, microbiologica, et immunologica Scandinavica* 96, 379-394 (1988).

98. Mitchell, W.K.*, et al.* Sarcopenia, dynapenia, and the impact of advancing age on human skeletal muscle size and strength; a quantitative review. *Frontiers in physiology* 3, 260 (2012).

99. McLoon, L.K. & Wirtschafter, J. Activated satellite cells in extraocular muscles of normal adult monkeys and humans. *Invest Ophthalmol Vis Sci* 44, 1927-1932 (2003).

100. Bankole, L.C., Feasson, L., Ponsot, E. & Kadi, F. Fibre type-specific satellite cell content in two models of muscle disease. *Histopathology* 63, 826-832 (2013).

101. Delhaas, T., Van der Meer, S.F., Schaart, G., Degens, H. & Drost, M.R. Steep increase in myonuclear domain size during infancy. *Anatomical record (Hoboken, N.J. : 2007)* 296, 192-197 (2013).

102. Legerlotz, K. & Smith, H.K. Role of MyoD in denervated, disused, and exercised muscle. *Muscle Nerve* 38, 1087-1100 (2008).

103. Hyatt, J.P., Roy, R.R., Baldwin, K.M. & Edgerton, V.R. Nerve activity-independent regulation of skeletal muscle atrophy: role of MyoD and myogenin in satellite cells and myonuclei. *American journal of physiology. Cell physiology* 285, C1161-1173 (2003).

104. Ishido, M., Kami, K. & Masuhara, M. In vivo expression patterns of MyoD, p21, and Rb proteins in myonuclei and satellite cells of denervated rat skeletal muscle. *American journal of physiology. Cell physiology* 287, C484-493 (2004).

105. Hyatt, J.P., Roy, R.R., Baldwin, K.M., Wernig, A. & Edgerton, V.R. Activity-unrelated neural control of myogenic factors in a slow muscle. *Muscle Nerve* 33, 49-60 (2006).

106. Bickel, C.S.*, et al.* Time course of molecular responses of human skeletal muscle to acute bouts of resistance exercise. *Journal of applied physiology (Bethesda, Md. : 1985)* 98, 482-488 (2005).

107. Kosek, D.J., Kim, J.S., Petrella, J.K., Cross, J.M. & Bamman, M.M. Efficacy of 3 days/wk resistance training on myofiber hypertrophy and myogenic

mechanisms in young vs. older adults. *Journal of applied physiology (Bethesda, Md. : 1985)* 101, 531-544 (2006).

108. Chen, C.M., Stott, N.S. & Smith, H.K. Effects of botulinum toxin A injection and exercise on the growth of juvenile rat gastrocnemius muscle. *Journal of applied physiology (Bethesda, Md. : 1985)* 93, 1437-1447 (2002).

109. Caiozzo, V.J., Wu, Y.Z., Baker, M.J. & Crumley, R. Effects of denervation on cell cycle control in laryngeal muscle. *Archives of otolaryngology--head & neck surgery* 130, 1056-1068 (2004).

110. Ma, J.*, et al.* Gene expression of myogenic regulatory factors, nicotinic acetylcholine receptor subunits, and GAP-43 in skeletal muscle following denervation in a rat model. *Journal of orthopaedic research : official publication of the Orthopaedic Research Society* 25, 1498-1505 (2007).

111. Otto, A.*, et al.* Canonical Wnt signalling induces satellite-cell proliferation during adult skeletal muscle regeneration. *J Cell Sci* 121, 2939-2950 (2008).

112. Comley, L.H., Nijssen, J., Frost-Nylen, J. & Hedlund, E. Cross-disease comparison of amyotrophic lateral sclerosis and spinal muscular atrophy reveals conservation of selective vulnerability but differential neuromuscular junction pathology. *The Journal of comparative neurology* 524, 1424-1442 (2016).

113. Liu, J.X., Brannstrom, T., Andersen, P.M. & Pedrosa-Domellof, F. Distinct changes in synaptic protein composition at neuromuscular junctions of extraocular muscles versus limb muscles of ALS donors. *PLoS One* 8, e57473 (2013).

114. Cisternas, P., Henriquez, J.P., Brandan, E. & Inestrosa, N.C. Wnt signaling in skeletal muscle dynamics: myogenesis, neuromuscular synapse and fibrosis. *Molecular neurobiology* 49, 574-589 (2014).

115. McLoon, L.K., Harandi, V.M., Brannstrom, T., Andersen, P.M. & Liu, J.X. Wnt and extraocular muscle sparing in amyotrophic lateral sclerosis. *Invest Ophthalmol Vis Sci* 55, 5482-5496 (2014).

116. Yin, Q.W., Johnson, J., Prevette, D. & Oppenheim, R.W. Cell death of spinal motoneurons in the chick embryo following deafferentation: rescue effects of tissue extracts, soluble proteins, and neurotrophic agents. *J Neurosci* 14, 7629-7640 (1994).

117. Harandi, V.M., Gaied, A.N.R., Brännström, T., Pedrosa Domellöf, F. & Liu, J. Unchanged Neurotrophic Factors and Their receptors Correlate with Sparing in Extraocular Muscles in Amoytrophic Lateral Sclerosis. *Invest Ophthalmol Vis Sci* (In press)(2016).

118. Maselli, R.A.*, et al.* Neuromuscular transmission in amyotrophic lateral sclerosis. *Muscle Nerve* 16, 1193-1203 (1993).

119. Liu, J.X., Brannstrom, T., Andersen, P.M. & Pedrosa-Domellof, F. Different impact of ALS on laminin isoforms in human extraocular muscles versus limb muscles. *Invest Ophthalmol Vis Sci* 52, 4842-4852 (2011).

120. Turner, M.R., Swash, M. & Ebers, G.C. Lockhart Clarke's contribution to the description of amyotrophic lateral sclerosis. *Brain* 133, 3470-3479 (2010).

121. Kanning, K.C., Kaplan, A. & Henderson, C.E. Motor neuron diversity in development and disease. *Annu Rev Neurosci* 33, 409-440 (2010).

122. Jacoby, J., Chiarandini, D.J. & Stefani, E. Electrical properties and innervation of fibers in the orbital layer of rat extraocular muscles. *J Neurophysiol* 61, 116-125 (1989).

123. Monemi, M., Kadi, F., Liu, J.X., Thornell, L.E. & Eriksson, P.O. Adverse changes in fibre type and myosin heavy chain compositions of human jaw muscle vs. limb muscle during ageing. *Acta physiologica Scandinavica* 167, 339-345 (1999).

124. Fahim, M.A., Holley, J.A. & Robbins, N. Topographic comparison of neuromuscular junctions in mouse slow and fast twitch muscles. *Neuroscience* 13, 227-235 (1984).

125. Somasekhar, T., Nordlander, R.H. & Reiser, P.J. Alterations in neuromuscular junction morphology during fast-to-slow transformation of rabbit skeletal muscles. *J Neurocytol* 25, 315-331 (1996).

126. Miles, J.D. & Cohen, M.L. Nerve and Muscle Biopsies. in *Neuromuscular Disorders in Clinical Practice* (eds. Katirji, B., Kaminski, H.J. & Ruff, R.L.) 235–260 (Springer Science+Business Media, New York, 2014).

127. Pedrosa-Domellof, F., Holmgren, Y., Lucas, C.A., Hoh, J.F. & Thornell, L.E. Human extraocular muscles: unique pattern of myosin heavy chain expression during myotube formation. *Invest Ophthalmol Vis Sci* 41, 1608-1616 (2000).

128. Maggs, A.M., Taylor-Harris, P., Peckham, M. & Hughes, S.M. Evidence for differential post-translational modifications of slow myosin heavy chain during murine skeletal muscle development. *Journal of muscle research and cell motility* 21, 101-113 (2000).

129. Maggs, A.M., Huxley, C. & Hughes, S.M. Nerve-dependent changes in skeletal muscle myosin heavy chain after experimental denervation and cross-reinnervation and in a demyelinating mouse model of Charcot-Marie-Tooth disease type 1A. *Muscle Nerve* 38, 1572-1584 (2008).

130. Thambisetty, M.*, et al.* Longitudinal changes in cortical thickness associated with normal aging. *Neuroimage* 52, 1215-1223 (2010).

131. Konigsmark, B.W. & Murphy, E.A. Neuronal populations in the human brain. *Nature* 228, 1335-1336 (1970).

132.   Vijayashankar, N. & Brody, H. A study of aging in the human abducens nucleus. *The Journal of comparative neurology* 173, 433-438 (1977).

133.   Vijayashankar, N. & Brody, H. Aging in the human brain stem. A study of the nucleus of the trochlear nerve. *Acta anatomica* 99, 169-172 (1977).

134.   Monagle, R.D. & Brody, H. The effects of age upon the main nucleus of the inferior olive in the human. *The Journal of comparative neurology* 155, 61-66 (1974).

135.   Sturrock, R.R. Stability of motor neuron number in the oculomotor and trochlear nuclei of the ageing mouse brain. *J Anat* 174, 125-129 (1991).